LUND UNIVERSITY

Master Thesis

Determination of Mass- and Heat Transfer Coefficients for Computer Modelling of Pharmaceutical Freeze-Drying

by

Linnea Gustafsson

Department of Food Technology, Engineering and Nutrition
Lund University
Sweden
June 7, 2021

Supervisors: **Professor Björn Bergenståhl,** **Doctor Anna Fureby**
Examiner: **Doctor Andreas Håkansson**

Front page picture: Scanning Electron Microscope (SEM) picture of freeze-dried cake (3% sucrose).

Postal address
PO-Box 124
SE-221 00 Lund, Sweden
Web address
www.food.lth.se

Visiting address
Getingevägen 60

Telephone
+46 46-222 83 05
+46 46-222 00 00

Printed in Sweden by Media-Tryck.
Lund 2021

Acknowledgement

This master thesis was carried out at the Department of Food Technology, Engineering and Nutrition at Lund University in collaboration with RISE Research Institutes of Sweden as a part of NextBioForm. With this project I conclude my master studies in Biotechnology Engineering at Lund University.

I would like to thank my supervisors Professor Björn Bergensthål and Anna Fureby, Director of NextBioForm at RISE, for exemplary mentorship and assistance throughout my thesis project. I have truly appreciated your support, and the time you have spent aiding me in my project. Your thoughts and theoretical and practical experience have been an invaluable contribution to the project, and I have learned much from both of you!

I would also like to say a big thank you to Shuai Bai, who has taken me on in addition to his ordinary supervisor duties. Your practical experience of freeze-drying has been crucial to the success of my experimental trials. Not to mention that your patience to discuss the sometimes incomprehensible results has continuously motivated me to seek new answers. The months working on my thesis project would not have been the same without you!

Finally, I would like to thank my examiner Doctor Andreas Håkansson for supporting my master thesis project.

Thank you!

Linnea Gustafsson 2021-05-26, Lund

Abstract

This thesis work deals with the determination of mass- and heat transfer coefficients for pharmaceutical vial freeze-drying and the one-dimensional steady state computer modelling of primary drying. The overall heat transfer coefficient K_V for the vial/freeze-dryer system was successfully determined using a gravimetric method. The overall resistance to mass transfer R_p was successfully determined for a 3% sucrose solution using a heat conduction model.

The pressure rise test with the manometric temperature algorithm was also investigated as an alternative method to monitor product temperature and determine transfer parameters without success.

A novel approach using an aluminum vial holder was evaluated as a method to increase temperature homogeneity during primary drying. When using the vial holder, vials situated at the center and edge of the freeze-dryer shelf did not differ in freeze-drying behaviour. It could also be shown that the vial holder increased heat transfer above 10 Pa, and decreased heat transfer below 2 Pa. However, additional investigation is required to fully understand the vial holder's effect on heat- and mass transfer parameters.

MATLAB was used to simulate primary drying of 3% sucrose solution at 10 Pa and -20°C based on determined K_V and R_p values. A one-dimensional steady state model based on governing mass- and heat transfer equations was used. When simulating primary drying of a full freeze-dryer shelf, the drying time was overestimated by 14%. Simulation of three vials placed in the vial holder instead underestimated the drying time with 9%. Predicted product temperatures were accurate for the first hours of primary drying, after which the accuracy significantly decreased. This is partly believed to be due to the phenomenon of microcollapse in the dry cake.

Sammanfattning

Detta examensarbete behandlar bestämningen av mass- och värmeöverföringskoefficienter för frystorkning av läkemedel i vialer, samt endimensionell steady state modellering av primärtorkning. Värmeöverföringskoefficienten K_V för den aktuella frystorken och vialen bestämdes framgångsrikt med en gravimetrisk metod. Massöverföringskoefficienten R_p bestämdes framgångsrikt för en 3% sackaroslösning med hjälp av en värmeledningsmodell.

Metoden kallad Pressure Rise Test, med Manometric Temperature (MTM) algortimen utvärderades som en alternativ metod för att bevaka produkttemperaturen och bestämma mass- och värmeöverföringskoefficienterna, utan framgång.

Ett nytt tillvägagångssätt, där en vialhållare av aluminium används under torkningen, utvärderades som metod för att minska temperaturskillnaden mellan vialer under primärtorkningen. När vialhållaren användes gick det inte längre att skilja på torkbeteendet för vialer i mitten och på kanten av frystorkningshyllan. Resultaten visar även att vialhållaren gav ökad värmeöverföring vid tryck över 10 Pa, och minskad värmeöverföring under 2 Pa. Ytterligare undersökningar behövs dock för att fullt förstå hur vialhållaren påverkar mass- och värmeöverföringen.

MATLAB användes för att simulera primärtorkningen av 3% sackaroslösning vid 10 Pa och -20°C, baserat på tidigare bestämda K_V och R_p värden. En endimensionell modell baserad på gällande mass- och energibalanser och antagande om steady state användes som modell. Simulering av en full hylla överskattade frystorkningstiden med 14%, medan simulering av 3 vialer placerade i vialhållaren underskattade torktiden med 9%. Modellen uppskattade produkttemperaturerna korrekt under de första timmarna av primärtorkningen, men inte under senare delen av torkningen. Detta tros delvis bero på att modellen inte beskriver händelsen av mikrokollaps korrekt.

Popular Science Abstract

In today's society, biopharmaceuticals are an essential part of many peoples lives. Vaccines, hormones, antibody therapies and insulin are examples of biopharmaceuticals that save lives and improve life quality every day. Today, biopharmaceuticals constitute about a third of all new pharmaceuticals. Nevertheless, the formulation and production of biopharmaceuticals comes with many challenges, where the stability of the active substance is the main issue. Often, biopharmaceuticals require gentle production methods, certain types of formulations, and demanding storage conditions to remain stable.

One such production method often used in the production of biopharmaceuticals is freeze-drying. Freeze-drying is a drying-technique where the product is dried by sublimation of ice from the frozen product. Freeze-drying is an essential part of many biopharmaceutical production processes. However, it is slow, energy demanding and expensive.

The aim of this thesis work is therefore to develop a computer based model for the drying process, to be used as support in process design and optimization of freeze-drying processes. If the drying process could be simulated with acceptable accuracy, some of the time consuming and expensive experimental work required to developing new freeze-drying processes could be avoided.

A prerequisite for modelling is that model parameters can be accurately determined. For this reason, a substantial part of this thesis work deals with the determination of mass- and heat transfer coefficients for the freeze-drying process.

In summary, this thesis work contributes to increased understanding of the freeze-drying process, how it can be modelled, and how model parameters for mass- and heat transfer can be determined.

Populärvetenskaplig sammanfattning

I dagens samhälle spelar biologiska läkemedel en stor roll i många människors liv. Vaccin, hormonläkemedel, antikroppsbaserade terapier och insulin är exempel på biologiska läkemedel som räddar liv och förbättrar människors livskvalitet varje dag. Idag är hela en tredjedel av alla nya läkemedel biologiska läkemedel. Att producera biologiska läkemedel innebär dock flera utmaningar, speciellt när det gäller stabiliteten av det verksamma ämnet i läkemedlet. Ofta kräver biologiska läkemedel extra skonsamma produktionsmetoder, speciella formuleringar och krävande förvaringsbetingelser för att inte förstöras.

En sådan produktionsmetod som ofta används vid tillverkning av biologiska läkemedel är frystorkning. Frystorkning är en torkmetod som går ut på att sublimera bort is från en fryst produkt. Frystorkning är tar lång tid, kräver mycket energi, och är dyrt. Trots detta är det en väsentlig del i många produktionsprocesser.

Syftet med detta examensarbete är därför att utveckla en modell för simulering av torkningen, som kan användas som support i processdesign och optimering av frystorkningsprocesser. Om torkprocessen kan modelleras med tillräcklig träffsäkerhet skulle det innebära att en del av det tidskrävande och dyra försöksarbetet som krävs för att designa en ny torkprocess kan undvikas.

En förutsättning för att kunna modellera är att modellparametrarna är korrekt bestämda. Därför ägnas en stor del av detta arbete till att hitta metoder för att bestämma mass- och värmeöverföringsparametrar för frystorkningsprocessen.

I sin helhet bidrar detta examensarbete till ökad förståelse för frystorkningsprocessen, hur den kan modelleras, samt hur modellparametrar för mass- och värmeöverföring kan bestämmas.

List of Symbols

A_p	product surface area, m^2
A_v	vial surface area, m^2
M	molecular mass of water, kg/mole
ΔH_{sub}	specific latent heat of sublimation, J/kg
K_c	heat transfer contribution from conduction, $W/m^2 \cdot K$
K_g	heat transfer contribution from convection, $W/m^2 \cdot K$
K_r	heat transfer contribution from radiation, $W/m^2 \cdot K$
K_V	overall heat transfer coefficient from heating fluid to bottom of vial, $W/m^2 \cdot K$
$K_{V,vh}$	overall heat transfer coefficient from vial holder to bottom of vial, $W/m^2 \cdot K$
K_1'	heat transfer coefficient between tray surface and bottom of vial, $W/m^2 \cdot K$
K_2'	heat transfer coefficient between shelf surface and tray bottom, $W/m^2 \cdot K$
K_S	heat transfer coefficient between heating fluid and shelf surface, $W/m^2 \cdot K$
L_D	thickness of dry layer, m
L_{frozen}	thickness of frozen layer, m
L_{tot}	total thickness of frozen and dry layer, m
L_{glass}	thickness of vial bottom, m
L_{tray}	thickness of tray, m
m	mass of sample in vial, kg
$\dot{m}$	sublimation rate of sample in vial, kg/s
m_{sub}	total mass of sublimated water of sample in vial, kg
P_C	chamber pressure, Pa
P_i	pressure at sublimation interface, Pa
$\dot{Q}$	heat flow rate, W
R_p	overall mass transfer coefficient, m/s
$R_{p,0}$	coefficient describing relationship between R_p and L_D, m/s
A_{R_p}	coefficient describing relationship between R_p and L_D, 1/s
B_{R_p}	coefficient describing relationship between R_p and L_D, 1/m

Greek letters

t	time, s
T_B	temperature at the inside bottom of the vial, °C
T_i	temperature at the sublimation interface, °C
T_S	shelf temperature, °C
T_{vh}	temperature in the vial holder, °C
ΔT	temperature gradient in the frozen layer, °C
V_{fill}	fill volume, m^3

α	coefficient describing relationship between K_V and P_C, $W/m^2 \cdot K$
β	coefficient describing relationship between K_V and P_C, $W/m^2 \cdot K \cdot Pa$
γ	coefficient describing relationship between K_V and P_C, 1/Pa
λ_{glass}	thermal conductivity of glass, $W/m \cdot K$
λ_{ice}	thermal conductivity of ice, $W/m \cdot K$
λ_{tray}	thermal conductivity of tray, $W/m \cdot K$
ρ_{ice}	density of water, kg/m^3
ρ_{water}	density of ice, kg/m^3
ϵ	volume fraction of ice

Abbreviations

PRT	Pressure Rise Test
MTM	Manometric Temperature Measurment
DPE	Dynamic Parameter Estimations
PRA	Pressure Rise Analysis

Contents

1 Introduction

1.1 Overview

Biopharmaceuticals are an essential part of many peoples lives. Vaccines, hormones, antibody therapies and insulin are examples of biopharmaceuticals that save lives and improve life quality every day. Today, biopharmaceuticals constitute about a third of all new pharmaceuticals. Nevertheless, the formulation and production of biopharmaceuticals comes with many challenges, where the stability of the active substance is the main issue. Often, biopharmaceutcials require gentle production methods, certain types of formulations, and demanding storage conditions to remain stable.

This is the main objective for NextBioForm. Through the NextBioForm reseach center, RISE conducts research with the aim to understand and develop new formulation and processing technology to meet the challenges of biopharmceutics production. (RISE 2020).

A common preservation method for biopharmaceuticals is freeze-drying. As freeze-drying is a slow and energy demanding process, the incentive to optimize the freeze-drying process is high for both for industrial and research purposes. This is why, as a part of NextBioForm, RISE aims to deepen the understanding and develop alternative methods for biopharmaceutical freeze-drying.

Freeze-Drying has long been recognised as a drying and preservation method for foods and organic substances. Since the 1890's it has been practiced at industrial scale, and during the 1950's it grew to become routinely used within both the food and pharmaceutical industries. Today, freeze-drying mostly finds its use in the pharmaceutical industry, where the high cost and energy demand of freeze-drying is more accepted than in the food-industry. (Franks and Auffret 2007). In the pharmaceutical industry, and especially for biopharmaceuticals, freeze-drying is appreciated compared to other drying techniques because of its gentle nature. Since freeze-

drying is carried out at very low temperatures, chemical and biochemical reactions during the drying process are minimized, and thus, product characteristics are well preserved. (Kharaghani et al. 2017; Franks and Auffret 2007). Common products where freeze-drying is used for long-term preservation is blood plasma, antibiotics, viruses, hormone solutions, serum, yeasts etc. (Kharaghani et al. 2017).

As freeze-drying is an essential step in many pharmaceutical processes, although slow and energy demanding, it is easy to understand the interest in minimizing freeze-drying cycle time and optimizing process parameters. (Kharaghani et al. 2017; Franks and Auffret 2007)

This thesis work deals with the determination of essential mass- and heat transfer parameters and computer modelling of freeze-drying. Being able to determine transfer parameters would aid the understanding of the freeze-drying process, facilitate experimental investigations and allow simulation of the freeze-drying process. Accurate simulation of a freeze-drying run would allow predicting drying behaviour and drying time, and has the potential of significantly reducing the time spent on experimental trials.

1.2 Aim and Project Scope

The aim of this thesis work is to:

- determine mass- and heat transfer parameters for the primary drying of vial freeze-drying.
- investigate the influence on heat- and mass transfer parameters of using an aluminium vial holder when freeze-drying.
- simulate primary drying in MATLAB using a one-dimensional steady state model based on determined mass- and heat transfer parameters. The accuracy of the model will be evaluated by comparing simulation results with experimental data.

Not included in the project scope is:

- aspects of freezing and secondary drying not directly related to the primary drying process.
- two- and three-dimensional, and non-steady state modelling of the drying process.

2 Background

The following chapter aims to give an understanding of the freeze-drying theory needed to interpret the results of this thesis work. First, the theoretical and practical principles of freeze-drying are be explained briefly. Secondly, the governing mass- and energy balance equations are explained with emphasis on heat- and mass-transfer coefficients and the experimental determination of these. Finally, a short introduction to modelling of freeze-drying is given.

2.1 Principle of Freeze-drying

Freeze-drying is a method to dry frozen materials by sublimation of the frozen solvent (usually water). The basic principal of freeze-drying is most easily explained with a phase diagram of pure water (figure 2.1):

A. The product is frozen at atmospheric pressure.

B. The pressure is decreased below the equilibrium vapour pressure to sublimate the ice.

C. The temperature is increased to optimize drying behaviour, and to remove residual water when ice sublimation is complete.

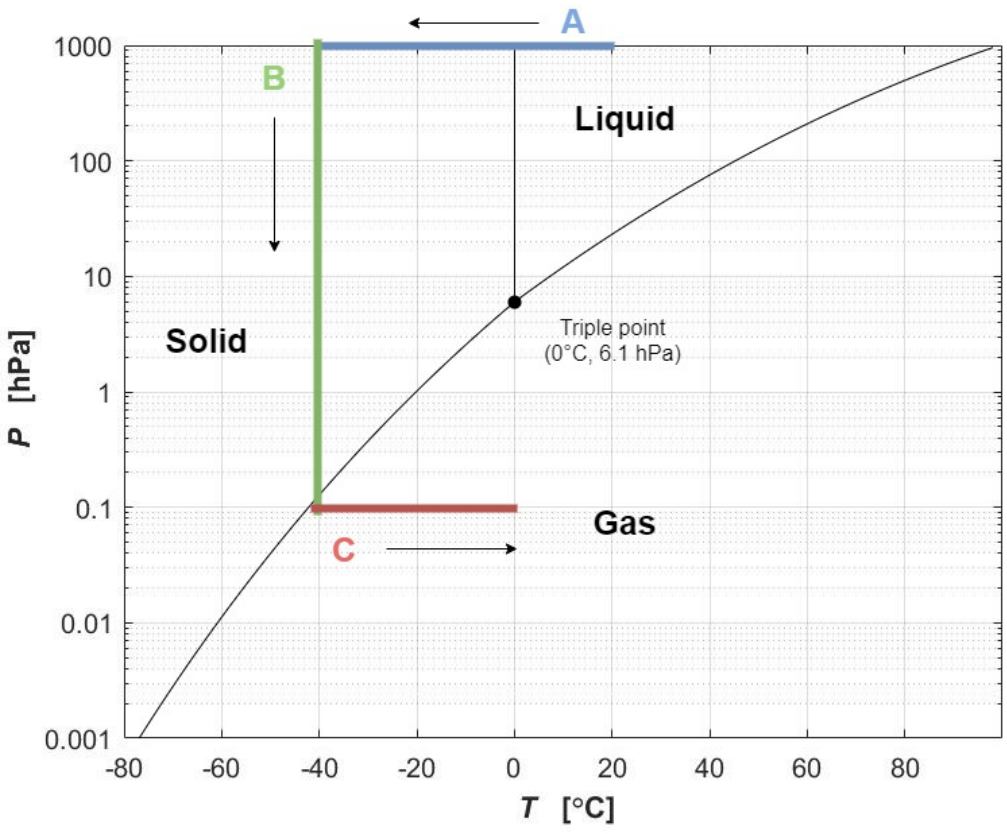

Figure 2.1 – Phase diagram of pure water with schematic representation of the freeze-drying principle. A: product is frozen at atmospheric pressure. B: Pressure is decreased below the equilibrium vapour pressure to start sublimation. C. Temperature is increased to optimize drying behaviour and to remove residual water once ice sublimation is completed.

2.2 Freeze-drying in Practice

The freeze-dryer consists of four main components schematically presented in figure 2.2:

- Drying chamber with temperature controlled shelves to supply the heat needed for sublimation of ice.
- Ice condenser to condense the water vapor evacuated from the drying chamber to ice. The condenser can be separated from the drying chamber by a vapor port.
- Vacuum pump to supply the vacuum needed to decrease pressure below the triple point.
- Compressor to cool the ice condenser and shelves in the drying chamber.

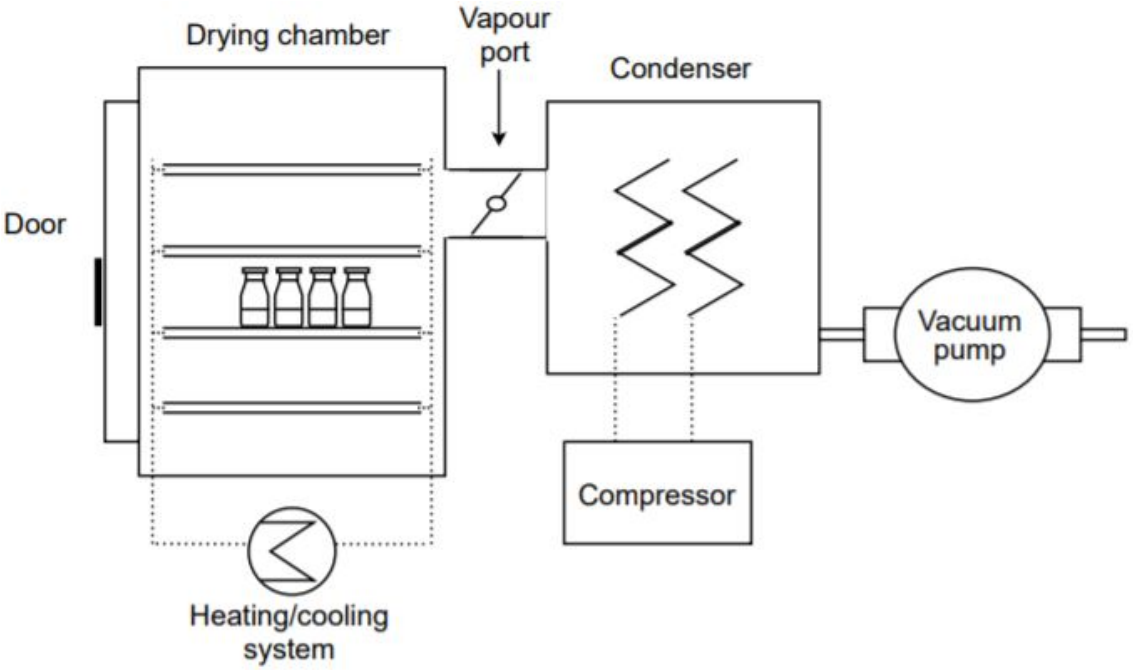

Figure 2.2 – Schematic representation of the main parts of a freeze-dryer.

When freeze-drying pharmaceuticals, the formulation can either be filled in vials, or poured into trays and placed on the freeze-dryer shelves. In this thesis work, only vial freeze-drying is concerned. The drying process itself is divided in three distinct phases:

1. Freezing, corresponds to A in figure 2.1.
2. Primary drying, refers to the sublimation of ice from the frozen product. It is conducted at pressures between 1-80 Pa and shelf temperatures between -40 and -5 °C. The heat needed for sublimation of ice is supplied from the temperature controlled shelves, and a dry layer evolves on top the frozen layer as more and more ice is sublimated. Corresponds to B in figure 2.1.
3. Secondary drying, refers to the removal of residual water from the dry layer by means of diffusion through the dry cake. In this stage, the temperature is gradually increased above 0 °C. Corresponds to C in figure 2.1.

A schematic representation of a vial during freeze-drying is shown in figure 2.3.

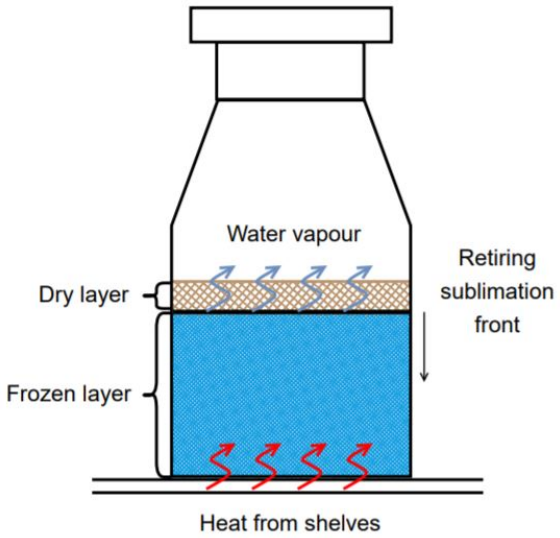

Figure 2.3 – Schematic representation of a vial during freeze-drying. Heat used for the sublimation of ice is supplied by the temperature controlled shelf. As more ice is sublimated, the sublimation moves towards the bottom of the vial.

2.2.1 Process Parameters

During freeze-drying, there are two main process parameters by which the drying process is controlled. The pressure in the drying-chamber and the temperature of the shelves.

The choice of operating conditions for a freeze-drying process is a balance between minimizing process time, and avoiding cake collapse and chocked flow. It is easy to believe that higher temperatures and lower pressures leads to higher product temperatures and faster drying. However, it is usually not that simple. As an example, lower pressure also leads to a decrease in heat transfer, since there is significantly less convection at very low pressures. As a result, lower pressure can sometimes lead to increased drying times instead of decreased. (Franks and Auffret 2007). Since in reality, the relationship between these process parameters, drying time and product temperatures is very complex, it is still often a case of trial and error to optimize a freeze-drying process. (Franks and Auffret 2007).

There are two main concerns which limit the drying process. Firstly, the temperature at the sublimation interface should in most applications not exceed the *collapse temperature*. At the collapse temperature, the pore structure of the dried layer is lost and the dry cake collapses and shrinks which causes unwanted cake appearance (Franks and Auffret 2007). For amorphous formulations, the collapse temperature is usually 1-2°C above the *glass transition temperature* (Kharaghani et al. 2017). As an example, for a 3-5% (w/w) sucrose solution the onset of collapse is observed around -35°C and complete collapse slightly above -34°C. (Fissore and Pisano 2015; Vanbillemont et al. 2020)

Secondly, the total vapour flow from the product being dried can not exceed the freeze-dryer's capacity to evacuate the vapour from the drying chamber. When this occurs, it is called *chocked flow*. Choked flow means loss of pressure control, limits the sublimation from the product, and causes increased product temperatures as less sublimation means higher temperature. This in turn also leads to collapse. (Patel, Chaudhuri, and Pikal 2010).

2.2.2 Process Monitoring

The most common method to monitor a freeze-drying run is with temperature and pressure sensors. The pressure is measured globally by two types of sensors placed in the drying chamber. *Capacitance* manometers measure the absolute pressure, while *Pirani* sensors are affected by the composition of the gas. They will always give a higher value than the capacitance manometer while there is water vapour in the drying chamber. Capacitance and Pirani sensors are often used in parallel, and the convergence between the capacitance and Pirani pressures can be used to determine the end of primary drying. (Kharaghani et al. 2017).

Temperature is monitored by placing thin temperature sensors called *thermocouples* in some vials. There are several problems with this method. When thermocouples are placed in the vials, they both act as an additional nucleation source, and conduct more heat to the vial. Thus, vials with thermocouples does not represent the other vials of the batch. Further, when the sublimation front moves past the placement of the thermocouple, it loses contact with the frozen product. At this point the temperature measurement stops being an accurate representation of the temperature in the frozen product. Despite disadvantages, using thermocouples is still the most common method to monitor product temperature. (Kharaghani et al. 2017)

In figure 2.4, a typical readout from a freeze-drying run where temperature and pressure have been measured is shown.

In recent years, several alternative process monitoring tools based on the pressure rise test (PRT) have been developed (Fissore, Pisano, and Barresi 2011b). A PRT is conducted by closing the valve between drying chamber and condenser for around 20 seconds, and recording the pressure rise in the drying chamber. By fitting the pressure rise data to an equation describing the pressure rise, the temperature at the bottom of the vial is estimated. Other parameters such as the temperature at the sublimation front, the overall heat transfer coefficient (see section 2.3.1) and dry layer resistance (see section 2.3.2) are also determined. In appendix A.3, the equations used by the Manometric Temperature Measurement (MTM) algorithm are presented. Other methods based on the PRT are the Pressure Rise Analysis (PRA) and Dynamic Parameter Estimation (DPE) algorithms.

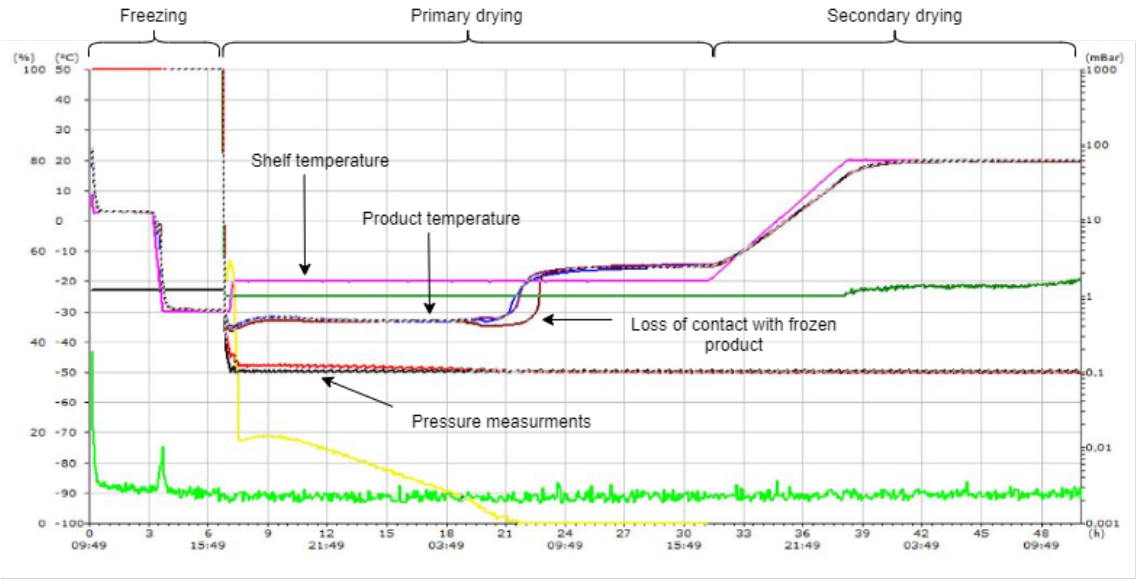

Figure 2.4 – Typical readout from a freeze-drying run where the pressure is measured with capacitance and Pirani pressure sensors, and the temperature with thermocouples in three vials.

An advantage with the methods based on the PRT is that they are non-invasive, and that the heat transfer coefficient and dry layer resistance can be monitored and determined in real time over the course of the entire drying period.

2.3 Governing Equations

Mass- and energy balance equations for vial freeze-drying are well described in literature, with most papers referencing the early works performed by Michael Pikal (1985) and Pikal, Roy and Shah (1984). They are built on the assumptions that:

- All heat transferred to the vial is used for the sublimation of ice, i.e. steady state and no heat accumulation in the frozen or dry layer is assumed.
- The retiring sublimation front is planar and with constant area. It moves perpendicular to the vial bottom, from the top of the frozen layer to the bottom of the vial.

Under the above assumptions, the mass balance during primary drying is described by equation 2.1 were $\dot{m}$ is the mass flow rate [kg/s]. A_p is the product surface area, based on the inner vial radius [m^2], P_i is the pressure at the sublimation interface, P_C the chamber pressure [Pa], and R_p the mass transfer coefficient describing the resistance to vapour flow [m/s].

$$\dot{m} = \frac{A_p}{R_p}(P_i - P_C) \tag{2.1}$$

The energy balance is described by equation 2.2, were $\dot{Q}$ is the heat flow rate [W], A_v the vial surface area based on the outer vial radius [m^2], T_S the temperature of the heating fluid in the shelf [K], T_B the product temperature at the bottom of the vial [K], and K_V the heat transfer coefficient [$W/m^2 \cdot K$].

$$\dot{Q} = A_v K_V (T_S - T_B) \tag{2.2}$$

During steady state conditions all energy supplied to the vial is used for sublimation of ice, and the mass- and energy balances can be coupled using equation 2.3, yielding equation 2.4, were ΔH_{sub} is the specific latent heat of sublimation [J/kg]. (Pikal, Roy, and Shah 1984; Fissore, Pisano, and Barresi 2011a; Tchessalov et al. 2021)

$$\dot{Q} = \Delta H_{sub} \dot{m} \tag{2.3}$$

$$A_v K_V (T_S - T_B) = \frac{\Delta H_{sub} A_p}{R_p} (P_i - P_C) \tag{2.4}$$

Since there is assumed to be no heat accumulation in the frozen layer, the thermal conductivity of ice λ_{ice} [W/m·K] and thickness of the frozen layer L_{frozen} [m] can be used to describe the temperature gradient over the frozen layer and relate the temperature at the bottom of the vial to the temperature at the sublimation interface using equation 2.5 (Pikal, Roy, and Shah 1984; Fissore, Pisano, and Barresi 2011a)

$$\left(\frac{1}{K_V} + \frac{L_{frozen}}{\lambda_{ice}} \right)^{-1} (T_S - T_i) = K_V (T_S - T_B) \tag{2.5}$$

In figure 2.5, a schematic representation of the mass- and energy balances during vial freeze-drying can be seen.

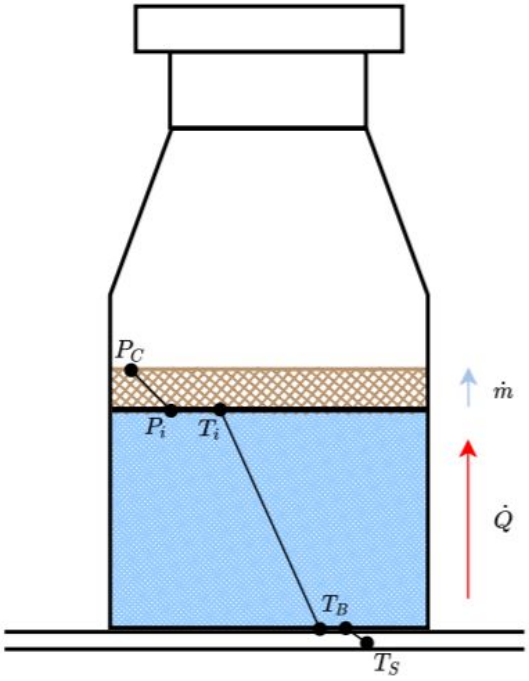

Figure 2.5 – Schematic representation of mass- and energy balances during vial freeze-drying with nomenclature used in this thesis work.

2.3.1 Heat Transfer Coefficient, K_V

The overall heat transfer coefficient K_V, is used to describe the dependence of heat flow to the vial on the driving temperature difference between the heating fluid in the shelf and the bottom of the vial. It is defined by equation 2.2 (Pikal 1985; Fissore, Pisano, and Barresi 2011a).

In case a tray is used between vials and shelf, the heat transfer from heating fluid to vial and the different components of K_V can be described by equation 2.6 (Pisano et al. 2013).

$$K_V = \frac{1}{\frac{1}{K_1'} + \frac{1}{K_2'} + \frac{L_{glass}}{\lambda_{glass}} + \frac{L_{tray}}{\lambda_{tray}} + \frac{1}{K_S}} \tag{2.6}$$

K_S is the heat transfer coefficient between the heating fluid inside the shelf and the shelf surface, K_2' is the heat transfer coefficient between the shelf surface and the tray surface, and $\frac{L_{tray}}{\lambda_{tray}}$ described the heat conductivity through the tray. K_1' is the heat transfer coefficient between tray surface and bottom of the vial, and finally $\frac{L_{glass}}{\lambda_{glass}}$ describes the conductivity through the vial bottom. If vials are placed directly on the shelf equation 2.6 can be simplified by removing components concerning heat transfer to the tray.

K_1' and K_2' can be expressed as the sum of three different heat transfer mechanisms according to equation 2.7 (Pikal, Roy, and Shah 1984).

$$K_1' = K_c + K_r + K_g \tag{2.7}$$

K_c is the contribution from the conduction at the points of direct contact between the tray surface and vial bottom, K_r is the contribution from radiation, and K_g is the contribution from conduction through the gas in the space between tray surface and vial bottom (Pikal, Roy, and Shah 1984). Because of the pressure dependence of K_g, K_V is mainly a function of the chamber pressure P_C and is described by equation 2.8 (Pikal 1985; Fissore, Pisano, and Barresi 2011a)

$$K_V = \alpha + \frac{\beta P_C}{1 + \gamma P_C} \tag{2.8}$$

α [W/m^2·K], β [W/m^2·K·Pa], and γ [1/Pa] are constants describing the pressure dependence of K_V. The value of α, β, and γ varies with the type of vial that is used, and the characteristics of the freeze-dryer (Pisano et al. 2013). They are most reliably experimentally determined (Fissore, Pisano, and Barresi 2011a).

In reality, and especially for lab- and pilot scale freeze-dryers, the heat transfer to the vial also receives contribution from the radiation from walls, door, other vials, and other shelves in the freeze-dryer (Pisano et al. 2013). As has been proposed in literature, the experimental measurement of an effective K_V will include these effects (Fissore, Pisano, and Barresi 2011a). However, heat transfer contribution from other sources than the dryer shelf poses a problem to both process control and process monitoring as it causes temperature heterogeneity within the dryer. The radiative heat transfer to a vial positioned in the middle of the dryer completely surrounded by other vials differs from the heat transfer to a vial positioned at the edge of a shelf close to the wall. This leads to differences in K_V and hence, differences in drying behaviour between vials in the same batch. This does not only complicate temperature control of the process, but results in different drying times for vials in the same batch. There are many examples in literature of attempts to minimize radiation effect. As an example, by covering the freeze-dryer door with aluminum foil (Tang, Nail, and Pikal 2006a).

Experimental Determination of K_V

The most common way of determining K_v is the gravimetric method. Vials are filled with solution, either a formulation or simply water, and then weighted before and after freeze drying. The temperature at the bottom of the vials is monitored using termocouples and in combination with the weight loss data, K_V is calculated using equation 2.9 where Δm is the weight difference [kg], and Δt is the time the vials have been dried [s] (Fissore, Pisano, and Barresi 2011a; Tang, Nail, and Pikal 2006c).

$$K_V = \frac{\Delta m \Delta H_{sub}}{\Delta t (T_S - T_B) A_V} \tag{2.9}$$

This method to determine K_V yields an average value for the entire drying time. However, K_V should not vary with drying time since the chamber pressure is kept constant. (Tang, Nail, and Pikal 2006c)

To determine the pressure dependence of K_V, freeze drying must be repeated for at least three different pressures, after which equation 2.8 can be fitted to the experimentally determined values of K_V versus P_C to determine constants α, β, and γ (Pisano et al. 2013).

The gravimetric method is time consuming compared to other methods, however it does not require any speciality equipment or software and it gives a picture of the heterogeneity of the drying behaviour as K_V can be determined for every single vial (Pisano et al. 2013).

Other methods for determining K_V are for example the use of tunable diode laser absorption spectroscopy (TDLAS) sensors, or with the different algorithms based on the pressure rise test (Bosca, Barresi, and Fissore 2013). Both of these methods require additional equipment or software.

2.3.2 Mass Transfer Coefficient, R_p

The mass transfer coefficient R_p describes the resistance to vapour flow and is used to model how the sublimation rate depends on the driving pressure difference $P_i - P_C$. Originally defined by Pikal et. al (1984), R_P referred only to the mass transfer resistance posed by the dry layer. Today, R_p is most often used as the term for the overall mass transfer resistance, which Pikal et. al. referred to as R_T, total mass transfer resistance (Fissore, Pisano, and Barresi 2011a; Pikal, Roy, and Shah 1984). The total mass transfer resistance is made up from three contributions; resistance from the dry product layer which evolves as the freeze-drying cycle proceeds, resistance from the stopper and vial neck, and resistance from the chamber and condenser. The dominating factor is by far the resistance from the dry product layer, and it is often stated that resistance from stopper and chamber can be neglected (Pikal, Roy, and Shah 1984; Bosca, Barresi, and Fissore 2013). From now on, R_p will refer to the overall resistance to mass transfer.

As the dry product layer evolves through the freeze-drying cycle, R_p changes. Therefore, R_p is commonly described as a function of the dry layer thickness L_D [m] according to equation 2.10. $R_{p,0}$ [m/s], A_{R_p} [1/s], and B_{R_p} [1/m] are coefficients determined by fitting equation 2.10 to experimental data.

$$R_p = R_{p,0} + \frac{A_{R_p} L_D}{1 + B_{R_p} L_D} \tag{2.10}$$

The resistance to mass transfer depends heavily on the structure of the frozen and dry layer. This means that R_p is formulation specific, as well as specific to the used freezing protocol (Pisano et al. 2013). For amorphous formulations, for example formulations containing sugars, R_p is also temperature dependent with decreasing R_p for higher shelf temperatures. This is attributed to the phenomenon of microcollapse. As the temperature at the sublimation interface approaches the glass transition temperature, some of the pore structure in the dry layer is lost. This results in the establishment of channels from the sublimation interface to the surface of the dry layer, making it easier for water vapour to flow through the dry layer. The higher temperature, the more microcollapse and lower R_p. (Fissore, Pisano, and Barresi 2011a; Kuu, Hardwick, and Aker 2006; Fissore and Pisano 2015).

In addition, the occurrence of microcollapse is also believed to cause the peculiarity of constant, or even decreasing R_p as primary drying progresses for amorphous formulations. For crystalline formulations R_p increases linearly as the dry layer thickness increases. However, for amorphous formulations, R_p values reaching a plateau are widely reported in literature (Bosca, Barresi, and Fissore 2013; Kuu, Hardwick, and Aker 2006).

It must be noted, that microcollapse is not to be mistaken for the large-scale collapse causing complete loss of pore structure and and unwanted cake appearance.

Experimental Determination of R_p

Unlike K_V, the resistance to mass transfer is not as straight forward to determine experimentally, since the driving force behind the mass transfer, $P_C - P_i$, is harder to measure. While P_C is known, the pressure at the sublimation interface P_i, cannot be directly measured in an environment similar to a real freeze-drying run. Adding to the challenge of estimating R_p accurately is the stochastic behaviour of the freezing-process, which causes vial-to-vial variability in R_p unless methods to control the freezing process are used (Pisano et al. 2013).

In this thesis work R_p was estimated using the heat conduction model in equation 2.5 to calculate the temperature at the sublimation interface by monitoring the product temperature at the bottom of the vial (Scutellà et al. 2018; Vanbillemont et al. 2020). This way of estimating R_p requires that K_V has already been determined. Since K_V is known, equation 2.11 can be used to estimate the temperature at the sublimation interface. L_{frozen} is the thickness of the frozen layer [m] and λ_{ice} is the thermal conductivity of ice [W/m·K].

$$T_i = T_B - \frac{(T_S - T_B)K_V L_{frozen}}{\lambda_{ice}} \tag{2.11}$$

From T_i, the pressure at the sublimation interface is estimated using equation 2.12, where A_{P_i}, B_{P_i}, C_{P_i}, and D_{P_i} are constants (Fissore, Pisano, and Barresi 2011a; Vanbillemont et al. 2020).

$$P_i = e^{A_{P_i} - \frac{B_{P_i}}{T_i} + C_{P_i} ln(T_i) - D_{P_i} T_i} \tag{2.12}$$

The sublimation rate at any given time during primary drying is calculated from equation 2.13, derived from equation 2.4.

$$\dot{m} = \frac{A_v K_V (T_S - T_B)}{\Delta H_{sub}} \tag{2.13}$$

Finally, R_p can be estimated from equation 2.14, also derived from equation 2.4.

$$R_p = \frac{A_p(P_i - P_C)}{\dot{m}} \tag{2.14}$$

The thickness of the dry layer at any given moment of the freeze-drying is calculated from the sublimation rate in equation 2.13, and coefficients $R_{p,0}$, A_{R_p}, and B_{R_p} are determined by fitting the experimentally estimated R_p and L_D values to equation 2.10.

Other methods to determine R_p are the algorithms based on the pressure rise test, with tunable diode laser absorption spectroscopy (TDLAS) sensors, from product temperature profiles, and by using a small weighing device in the freeze-dryer to measure mass-loss in real time (Fissore, Pisano, and Barresi 2011a). All these methods require additional speciality equipment or software (Bosca, Barresi, and Fissore 2013).

2.4 Computer Modelling

Computer modelling of primary drying has long been practiced with the goal of aiding understanding of process parameters and shortening experimental trials and process design (Pikal 1985; Tchessalov et al. 2021).

There are a number of primary drying models, all building on the basic understanding of governing mass- and energy balance equations provided by Pikal et.al. during the 1980's. The main difference between models is if they are one- or two-dimensional and whether they assume steady state or not. (Tchessalov et al. 2021).

Even if the understanding of freeze-drying processes and governing equations is relatively good, modeling relies on accurately determined model parameters describing the process adequately to be useful (Fissore, Pisano, and Barresi 2011a). This sometimes proves difficult, since there is an intrinsic vial-to-vial and batch-to-batch variability, and since mass- and heat transfer parameters change as formulation, vial type and process parameters change. (Fissore, Pisano, and Barresi 2011a; Pisano et al. 2013).

With the Quality By Design approach gaining ground in the pharmaceutical industry, computer modelling of pharmaceutical freeze-drying has also taken a new approach. Today, the aim of much published freeze-drying research is to develop simulation based tools to establish the design space for a freeze-drying cycle. (Fissore, Pisano, and Barresi 2011a; Pisano et al. 2013; Mortier et al. 2016)

3 Materials and Methods

All freeze-drying experiments described below were carried out in a Martin Christ Epsilon 2-6D LSC Plus freeze-dryer using Schott VCDIN8R tubing vials and West silicone stoppers (FDW20RTS). Type T thermocouples from Martin Christ (Art.no: 124799) were used to monitor product temperature. Capacitance and Pirani pressure sensors were used to monitor the chamber pressure. Values for all constants and parameters used in the study can be found in table 3.1.

To counteract the problem of temperature heterogeneity within the freeze-dryer an aluminium vial holder was used in some of the experiments. The purpose for using the vial holder was both to increase the temperature control, and to evaluate the difference between the set-ups with, and without vial holder. The holder (figure 3.1) had previously been design and manufactured at the Department of Food Technology, Engineering and Nutrition, and consists of a solid aluminum block with drilled holes for 54 vials (⌀ 22 mm), as well as smaller holes for the placement of thermocouples.

(a) **(b)**

Figure 3.1 – (a) Vial holder with 54 vials and inserted thermocouples. Note the small holes in the aluminium block for placement of thermocouples. (b) Vial holder with 54 vials and inserted thermocouples placed on the middle and bottom shelves of the freeze-dryer.

3.1 Determination of Heat Transfer Coefficient, K_V

The gravimetric method described in 2.3.1 was used to determine the overall heat transfer coefficient, K_V, when vials were placed directly on the shelf, and when the vial holder was used.

54 vials were filled with 4 ml of deionized water and semi-stoppered before each vial was weighed using an analytical scale. The vials were then placed on the middle shelf of the freeze-dryer, either in the vial holder, or directly on the shelf with the same positioning of the vials as in the vial holder. Termocouples were placed in three of the vials to measure the product temperature at the bottom of the vials. The positioning of the vials with termocouples can be seen in figure 3.2. During one run were the vial holder was used, a thermocouple was placed in the vial holder as well, to be able to measure the temperature in the holder during the experiment.

The vials were frozen and subjected to 2 hours of primary drying before the freeze-drying was terminated. The following freeze-drying protocol was used: *1.* freezing at atmospheric pressure from 20 °C to -45 °C at a rate of 2.2 °C/min. *2.* hold at -45 °C for 20 min. *3.* decrease pressure to the desired vacuum over a period of 10 minutes. *4.* raise the temperature to -15°C at a rate of 3 °C/min. *5.* hold -15°C and desired vacuum for 2 hours. After drying, the vials were stoppered immediately and allowed to return to ambient temperature before each vial was re-weighted. From the weight difference and measured product temperature K_V for each vial was calculated using equation 2.9. The average product temperature for the three vials with thermocouples was used as T_B for all vials.

To determine the pressure dependence of K_V, freeze-drying was carried out at 6 different chamber pressures with vial holder (3.125, 6.25, 10, 12.5, 25, and 50 Pa), and at 5 different pressures without vial holder (3.125, 6.25, 12.5, 25, and 50 Pa). During one of the runs at 10 Pa with the vial holder, a thermocouple was placed in the vial holder as well as in the vials. The constants α, β, and γ were determined for each case by fitting equation 2.8 to the experimental data using MATLAB R2020a and the fit function from the curve fitting toolbox.

To determine if there was any significant difference between the heat transfer to the edge vials and to the non-edge vials, the vials were divided into two groups, *edge vials* and *non-edge vials*. The groups are visualized in figure 3.2. The mean K_V of each group were then compared using a two sided T-test.

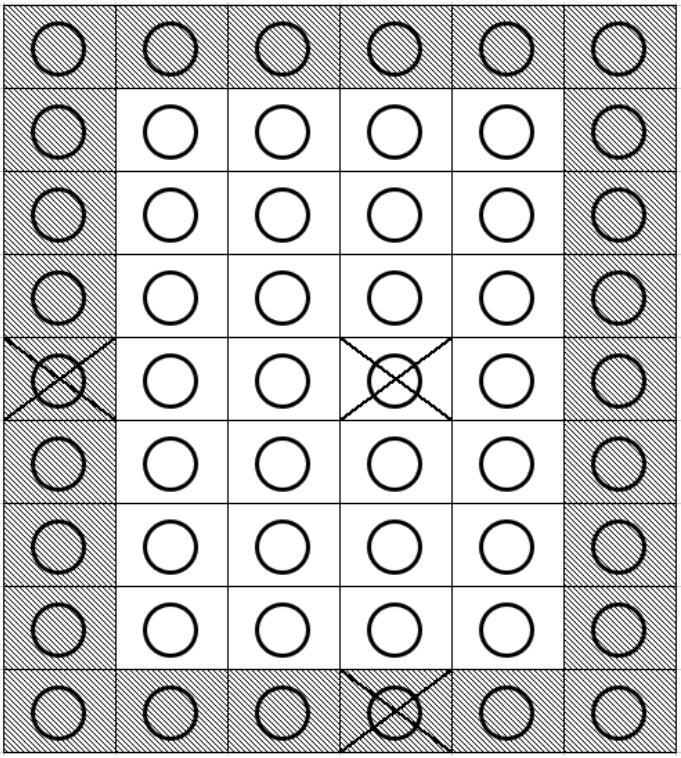

Figure 3.2 – Schematic representation of the placement of the vials on the freeze-dryer shelf. The vials were placed either directly on the shelf, or in a vial holder. The shaded vials are the *edge vials* and the transparent vials are the *non-edge vials*. The crosses are vials with thermocouples.

3.2 Determination of Mass Transfer Coefficient, R_p

To estimate R_p, vials were filled with 3 ml of a 3% (w/w) sucrose solution and freeze-dried with the following freeze drying protocol. *1.* Equilibrate at 3°C for 3 hours *2.* Lower temperature to -30°C at a rate of 1°C/min *3.* Hold at -30°C for 3 hours. *4.* Adjust vacuum to 10 Pa in 10 minutes *5.* Increase temperature to -20°C at a rate of 1°C/min *6.* Hold -20°C and 10 Pa until primary drying is completed. *7.* Increase temperature to 20 °C at a rate of 0.1 °C/min. *8.* Hold at 20°C.

Comparative pressure measurement between the capacitance and pirani pressures was used as a progress condition for the primary drying, with a limit value of 3%. The product temperature at the bottom of the vial was monitored by thermocouples in three non-edge vials. R_p was determined with three different set-ups:

- 2 runs with 54 vials placed directly on the shelf, with the same positioning of the vials as in the vial holder. This is the set-up most resembling a standard freeze-drying run.
- 5 runs with 3 vials placed in the vial holder, with thermocouples in all three vials. 5 runs were performed to estimate the variability of R_p. The reason for only using vials with thermocouples was to accurately be able to determine the end of primary drying for *all* vials in the freeze dryer and compare to simulations of the primary drying.
- 1 run with 54 vials placed in the vial holder, to be able do distinguish between the effect of the number of vials and the vial holder in the previous two set-ups.

From the temperature measurements and previously determined K_V for the appropriate conditions (see table 4.1), equations 2.11-2.14 where used to estimate R_p and L_D. Note that the average temperature from the three thermocouples, up to the point where they loose contact with the frozen layer, was used as T_B.

Constants $R_{p,0}$, A_{R_p}, and B_{R_p} were then determined by fitting the R_p and L_D estimations to equation 2.10. MATLAB R2020a and the lsqcurvefit function for non-linear regression in the optimization toolbox was used for fitting. The complete MATLAB function script to determine R_p can be found in Appendix A.2.

3.3 PRT for K_V and R_p determination

As an alternative method to estimate both K_V and R_p non-invasively, the pressure rise test with the MTM algorithm was evaluated.

Vials were treated in the same manner as described in section 3.1 Determination of Heat Transfer Coefficient, and pressure rise tests were performed every 30 minutes during the 2 hour primary drying time.

3.4 Vial Holder Temperature

Since there was a suspicion that the number of vials in the vial holder affected the temperature in the vial holder, two measurements of vial holder temperature were made. One with 3 vials in the vial holder, and one with 54 vials in the vial holder. The vials were treated as described in the previous section 3.2 Determination of Mass Transfer Coefficient, R_p, except from that two of the thermocouples were placed in vials, and one in the vial holder.

3.5 Computer Model

A simple mechanistic model derived from the governing mass- and energy balance equations (2.1-2.4) was used to simulate the primary drying of a freeze-drying cycle. The model describes the evolution of the dry layer thickness during primary drying and has previously been outlined in literature by Mortier et. al. (2016) and Vanbillemont et.al. (2020). Note that as it is based on the mass- and energy balance equations the model is built on the same underlying assumptions.

From a set of operating conditions (shelf temperature T_S, chamber pressure P_C, and filling volume V_{fill}) the model calculates the pressure and temperature at the sublimation interface P_i and T_i, the temperature difference across the frozen layer ΔT, and the specific latent heat of sublimation ΔH_{sub} at every time step. When this is known, the thickness of the dry layer as a function of time can be calculated. When the thickness of the dry layer L_D equals the total thickness L_{tot} the primary drying is completed.

The model consists of the four equations 3.1-3.4 which must be solved simultaneously as they are interdependent (Mortier et al. 2016; Vanbillemont et al. 2020).

$$P_i = \frac{A_p \Delta H_{sub} P_c + A_v K_v R_p T_s - A_v K_v R_p T_i - A_v K_v R_p \Delta T}{A_p \Delta H_{sub}} \tag{3.1}$$

$$\Delta T = \frac{a \frac{(L_{tot} - L_D)(P_i - P_c)}{R_p} - b(L_{tot} - L_D)(T_s - T_i)}{1 - b(L_{tot} - L_D)} \tag{3.2}$$

$$\Delta H_{sub} = \frac{A_{H_{sub}} + B_{H_{sub}} T_i - C_{H_{sub}} T_i^2 + D_{H_{sub}} e^{-(\frac{T_i}{E_{H_{sub}}})^2}}{M} \tag{3.3}$$

$$P_i = e^{A_{P_i} - \frac{B_{P_i}}{T_i} + C_{P_i} ln(T_i) - D_{P_i} T_i} \tag{3.4}$$

Equation 3.1 is a rearrangement of the coupled mass- and energy balance in equation 2.4 and equation 3.2 is a combination of the mass- and energy balances and the heat transfer through the frozen layer by means of thermal conductivity. a and b are constants to convert to SI-units (Tang, Nail, and Pikal 2006b; Pikal 1985). Equations 3.3 and 3.4 are equations describing the dependence of the specific latent heat of sublimation of ice ΔH_{sub} (Murphy and Koop 2005) and the equilibrium vapour pressure over ice, P_i (Fissore, Pisano, and Barresi 2011a; Vanbillemont et al. 2020) on the temperature at the sublimation interface T_i.

When P_i is known the sublimation rate $\dot{m}$ is calculated using:

$$\dot{m} = \frac{A_p(P_i - P_c)}{R_p} \tag{3.5}$$

The total mass of sublimated ice is given by:

$$m_{sub,t+1} = m_{sub,t} + \dot{m}_{sub,t}\Delta t \tag{3.6}$$

where Δt [s] is the time-step used in the iteration. Finally, the thickness of the dry layer at a given moment can be calculated from:

$$L_D = \frac{m_{sub}}{A_p \rho_{ice} \epsilon} \tag{3.7}$$

where ρ_{ice} [kg/m^3] is the density of ice and ϵ [-] is the volume fraction of ice in the frozen layer. The total thickness of both frozen and dry layer is calculated from the filling volume V_{fill} [m^3]:

$$L_{tot} = \frac{V_{fill} \rho_{water} \epsilon}{A_p \rho_{ice}} \tag{3.8}$$

where ρ_{water} [kg/m^3] is the density of water.

MATLAB R2020a with the optimization toolbox was used to simulate the primary drying. More specifically, the fsolve function for solving non-linear equation systems was used to solve equations 3.1-3.4. The complete model MATLAB-script can be found in Appendix A.1. The values for constants used in the model are presented in table 3.1.

To estimate how much the model prediction of primary drying time differed from reality (due to thermocouple effects), simulations were performed with the R_p values determined from the two runs with 54 vials placed directly on the shelf described in section 3.2. The prediction of primary drying time was then compared to the real drying time for these runs.

3.6 Model Verification

In order to asses the accuracy of the freeze-drying model, the following two cases were simulated and compared to verification runs:

- 54 vials placed directly on the shelf. K_V from table 4.1 for non-edge vials and R_p from table 4.2 for 54 vials without vial holder was used.
- 3 vials placed in the vial holder. K_V from table 4.1 for vials in vial holder and R_p from table 4.2 for 3 vials in vial holder was used.

During both verification runs, three thermocouples were placed in center vials to monitor product temperature at the vial bottom (i.e during the run with 3 vials, all vials had thermocouples). The end of primary drying was determined by comparative pressure measurement with a limit value of 3%.

The accuracy of the simulation was estimated by comparing the predicted product temperature and time of primary drying with the verification run.

3.7 Constants and Parameters

Table 3.1 – Constants, vial characteristics, physical properties and coefficients used in the simulation of primary drying and R_p-determination.

Constant	Value	Unit	Description
A_p	3.8013 x 10^{-4}	m^2	product surface area
A_v	4.5239 x 10^{-4}	m^2	vial surface area
a	889200	-	factor for conversion to SI units
b	0.0102	-	factor for conversion to SI units
$A_{H_{sub}}$	4.68 x 10^4	J/mol	coefficient for calculation of ΔH_{sub}
$B_{H_{sub}}$	35.9	J/mol· K	coefficient for calculation of ΔH_{sub}
$C_{H_{sub}}$	0.0741	J/mol· K^2	coefficient for calculation of ΔH_{sub}
$D_{H_{sub}}$	542	J/mol	coefficient for calculation of ΔH_{sub}
$E_{H_{sub}}$	124	K^2	coefficient for calculation of ΔH_{sub}
A_{P_i}	9.550426	Pa	coefficient for calculation of P_i
B_{P_i}	5723.2658	K	coefficient for calculation of P_i
C_{P_i}	3.53068	1/K	coefficient for calculation of P_i
D_{P_i}	0.00728332	Pa	coefficient for calculation of P_i
M	0.0180	kg/mol	molecular mass of water
ρ_{ice}	998.2	kg/m^3	density of water
ρ_{water}	919.5	kg/m^3	density of ice
ϵ	0.97	-	volume fraction of ice
Δt	5	s	time step used in calculations and simulation

4 Results and Discussion

4.1 Determination of K_V

The overall heat transfer coefficient K_V was successfully determined at all the tested pressure levels. The mean K_V at every pressure level and the resulting equation fit for freeze-drying both with and without vial holder is presented in figure 4.1. The values for α, β, and γ can be found in table 4.1

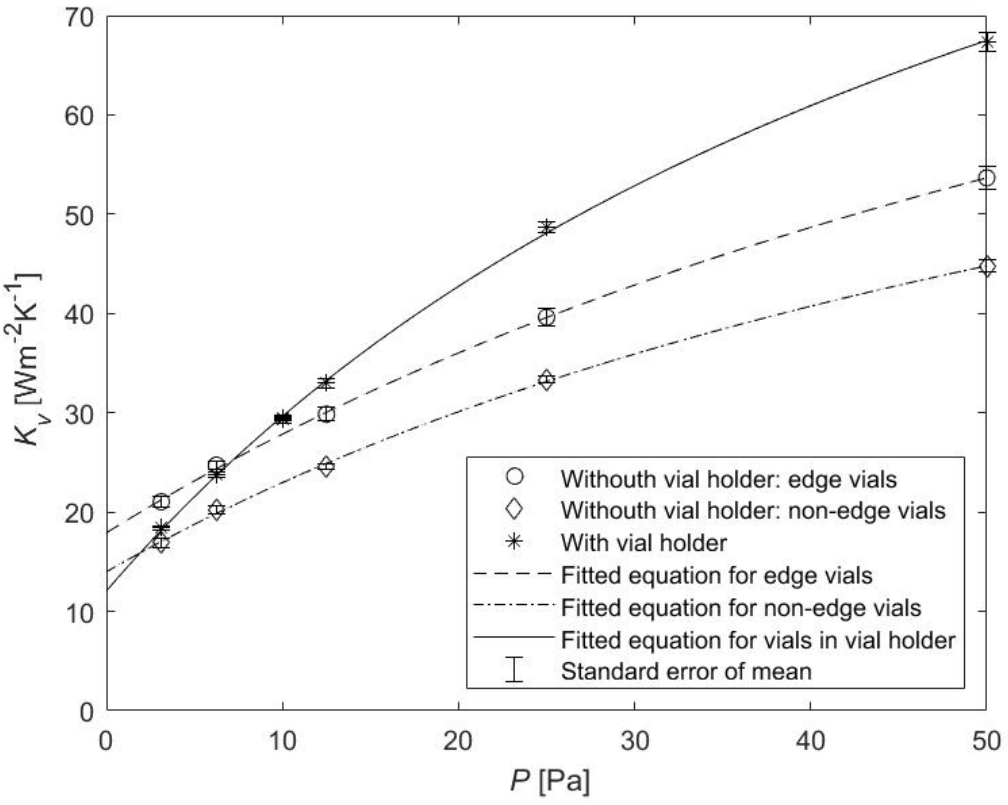

Figure 4.1 – Overall heat transfer coefficient K_V versus chamber pressure P_C. K_V was determined from gravimetric measurements and by monitoring product temperature at the bottom of the vials. Presented K_V values are the average values for the different groups of vials. The curves are determined from fitting experimental data to equation 2.8.

At all five pressure levels it was possible to distinguish between the mean K_V value for the *edge vials* and the *non-edge vials* with a two sided t-test at 95% confidence level when the vials were placed directly on the shelf. This was mostly due to the fact that the edge vials close to the door had significantly higher K_V than the rest of the vials. This indicates that another grouping than edge and non-edge vials might represent the temperature heterogeneity better. The results regarding both the magnitude of K_V, and the difference between edge and non-edge vials for the case without vial holder are very similar to results reported in literature (Vanbillemont et al. 2020; Pisano et al. 2013; Mortier et al. 2016).

When the vial holder was used, it was not possible to distinguish between the two groups at any of the pressure levels. The standard deviation in K_V was also slightly lower, than for the case without vial holder. This indicates increased temperature homogeneity, and by extension, that a more homogeneous drying behaviour is achieved by using the vial holder. The reason that the standard deviation in K_V is only slightly lower when using the vial holder is that the variation in the centre vials seems to increase when using the vial holder. This is illustrated in figure 4.2. A reason for this could be uneven heat transfer to vials due to size-differences between vials yielding differences in how good the contact is between vial and vial holder.

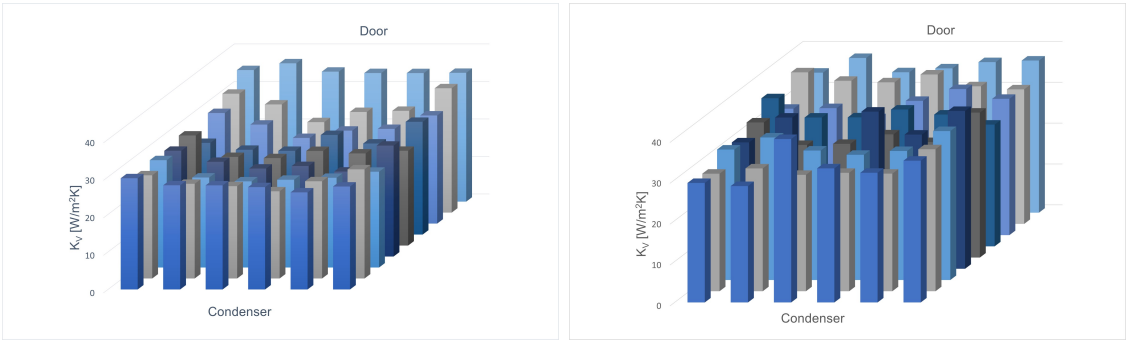

No vial holder, $\sigma = 3.7$ Vial holder, $\sigma = 3.2$

Figure 4.2 – Comparison of temperature heterogeneity when vials are freeze-dried at 12.5 Pa and -15 °C with and without vial holder. Each bar represents K_V of the vial at that position in the freeze-dryer. The standard deviation of K_V for the two cases is also displayed.

Above 10 Pa the heat transfer when using the vial holder is clearly higher than for both vial groups when placing vials directly on the shelf. However, below 7.3 Pa the heat transfer is highest for the *edge vials* without vial holder, and below 2 Pa even the heat transfer to the *non-edge vials* is higher than the heat transfer to the vials in the vial holder. This is most likely due to several factors. Firstly, it seems that K_V is more pressure sensitive when using the vial holder. This is not strange, since the area for heat conduction through gas (K_c) in increased to also include the space between the vial holder and the walls of the vial. Secondly, the radiation contribution, K_r at lower pressure were the conduction through gas, K_c, is less dominant plays a part. Vials not shielded by the aluminium holder, and especially the *edge vials* which are closest to the walls and doors of the freeze-dryer receive more radiative heat transfer.

Table 4.1 – Values for coefficients α, β, and γ describing the relationship between overall heat transfer coafficient K_V and chamber pressure P_C according to equation 2.8. Determined by fitting experimental data to the equation.

Case	α [W/m^2· K]	β [W/m^2· K· Pa]	γ [1/Pa]
With vial holder	12.1	2.06	0.017
Edge vials without vial holder	17.9	1.10	0.011
Non-edge vials without vial holder	14.0	1.01	0.013

4.2 Determination of R_p

The resistance to vapour flow, R_p, and its dependence on dry layer thickness, L_D, was successfully determined for all three set-ups described in section 3.2. In figure 4.3 one representative example from each set-up is shown of the R_p versus L_D estimations and the resulting fit to equation 2.10.

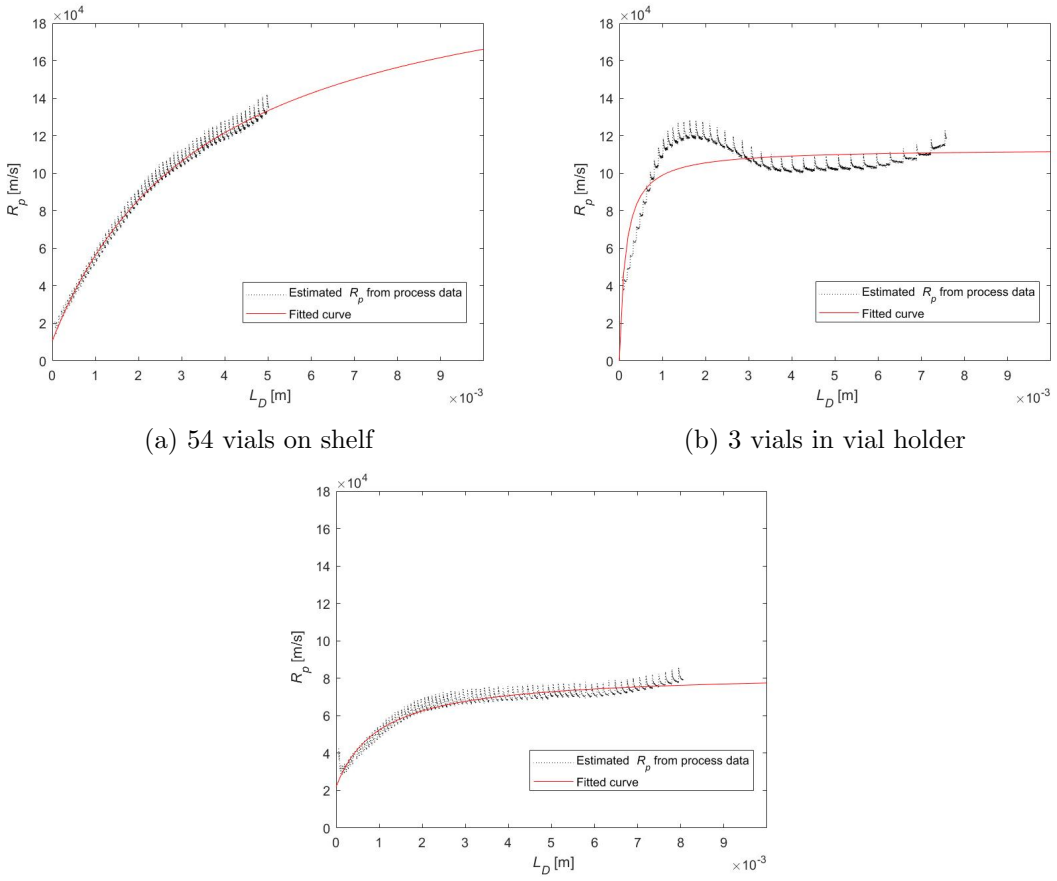

(a) 54 vials on shelf

(b) 3 vials in vial holder

(c) 54 vials in vial holder

Figure 4.3 – Estimated R_P versus L_D and resulting fit to equation 2.10 for three experimental set-ups. Vials were filled with 3 ml 3% (w/w) sucrose solution and freeze-dried at 10 Pa and -20°C. Dotted line is estimated R_p from product temperature measurement and red line is the fitted equation.

A first thing to note is the different shapes of the R_p curves. In the cases vial holder was used (with 3 and 54 vials), R_p assumes a constant value when the thickness of the dry layer reaches around 2 mm. When vials were placed directly on the shelf, R_p continuous to increase (although with decreasing slope) as L_D increases. These results correspond well with R_P values reported in literature for similar cases.

For example, for 3% sucrose solutions, with the same process conditions and similar freezing protocol as in this thesis work, similar results have been reported by Vanbillemont et. al (2020) and Kuu et. al (2006). Vanbillemont used the same method to estimate R_p as has been done in this report, and Kuu used temperature profiles. Kuu et. al even observed decreasing temperature and R_p for a 3% sucrose formulation, similar to what can be seen in figure 4.3b. According to the theory of microcollapse causing constant or decreasing R_p, the behaviour of R_p observed in figure 4.3b must mean that once channels have been established, R_p decreases, and then does not increase significantly as a result of increased dry layer thickness.

In support of this explanation, more collapse was observed in the cases vial holder was used, with the most collapse seen for 3 vials in vial holder (figure 4.4). This is also the set-up which gave the higher product temperature (figure 4.5). However, there is one problem with this reasoning. Higher product temperature and more microcollapse/collapse should yield a lower R_p, and while this is true for the case with 54 vials without vial holder compared to the cases were vial holder is used, it is not true when the two cases with vial holder are compared against each other. The case with 3 vials in the vial holder had the highest product temperature, and most visible collapse, however, the R_p is higher than for 54 vials in the vial holder. A possible explanation for this, is that the heat conduction model used to estimate R_p does not accurately describe the situation when the vial holder is used. This is discussed in more detail in section 4.4.

54 vials without vial holder | 54 vials in vial holder | 3 vials in vial holder

Figure 4.4 – Comparison between observed cake collapse for a 3% (w/w) sucrose solution freeze-dried at 10 Pa and -20°C with three different experimental set-ups. Observe the shrinkage of the cake.

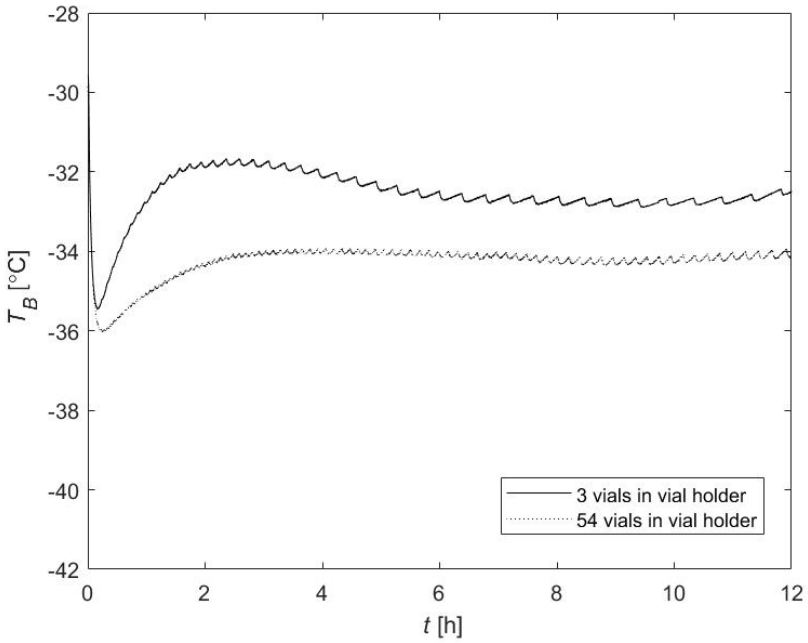

Figure 4.5 – Product temperature at the bottom of the vial during primary drying for experimental set-ups with 3 vials in vial holder and 54 vials in vial holder. Vials were freeze-dried at 10 Pa and -20°C according to section 3.2.

Another explanation for the difference in R_p curve shape is that the vial holder had an effect on the freezing behaviour, causing a differences in ice crystal structure. Even though it is likely that the vial holder affected the freezing behaviour in some way, there is no measurable evidence of this. For example, differences in undercooling at the crystallisation moment can affect the ice crystal structure, but no such difference was seen during the experiments.

A comment must be made on the fit of experimental data to equation 2.10. In figure 4.3b were a maximum R_p followed by a decrease is observed, the proposed equation 2.10 describing the relationship between R_p and L_D does not seem accurate. There are examples in literature using more sophisticated fitting algorithms than in this study, where the coefficient A_{R_p} is found to be negative for formulations which exhibit this phenomenon. While these fits represents the decreasing part of the R_p curve well, the overall fits are still bad (Kuu, Hardwick, and Aker 2006). An alternative method would be to describe the relationship between R_p and L_D in cases were microcollapse occurs with two intervals, performing one fit for each interval. One for the increasing part of the R_p versus L_D curve, and one for the decreasing/constant part.

Values of $R_{P,0}$, A_{R_p}, and B_{R_p} determined from fitting experimental data to equation 2.10 for the three set-ups are presented in table 4.2. In the cases were more than one freeze-drying run was performed, the the mean value of $R_{P,0}$, A_{R_p}, and B_{R_p} is displayed. The corresponding R_p versus L_D curves are presented in figure 4.6.

Table 4.2 – Experimentally determined values for $R_{p,0}$, A_{R_p}, describing the relation between R_p and dry layer thickness, L_D, for a 3% (w/w) sucrose solution freeze-dried at 10 Pa and -20°C. The values for 54 vials without vial holder are mean values from two runs. The values for 3 vials with vial holder are mean values from five runs.

Experimental set-up	$R_{p,0}$ [m/s]	A_{R_p} [1/s]	B_{R_p} [1/m]
54 vials without vial holder	$1.4{\cdot}10^4$	$5.8{\cdot}10^7$	$0.28{\cdot}10^2$
3 vials with vial holder	0.06	$6.0{\cdot}10^8$	$5.3{\cdot}10^3$
54 vials with vial holder	$2.2{\cdot}10^4$	$6.0{\cdot}10^7$	$0.98{\cdot}10^2$

To compare the R_p results to other studies, R_P versus L_D curves determined in four different studies with relevant formulations and process conditions are shown in figure 4.7. It is difficult to compare the exact values between different studies, since there are differences in the formulations, process conditions, freezing protocols, and freeze-driers used. However some things can be said. Firstly, the R_p results obtained in this study are comparable to those found in literature in both magnitude and curve shape. Secondly, all values found in literature have $R_{p,0}$ significantly higher than 0, around 1-4·10^4 m/s. This is reasonable, as one can imagine $R_{p,0}$ corresponding to an initial resistance, not produced by the dried layer, but due to the resistance to vapour flow from vial neck, stopper, condenser, and water. As can be seen in table 4.2, the set-ups with 54 vials without vial holder and 54 vials with vial holder compares well to this, however, 3 vials in vial holder yielded $R_{p,0} = 0.06$ m/s. This is not reasonable, and likely a result of the bad curve fitting observed in figure 4.3.

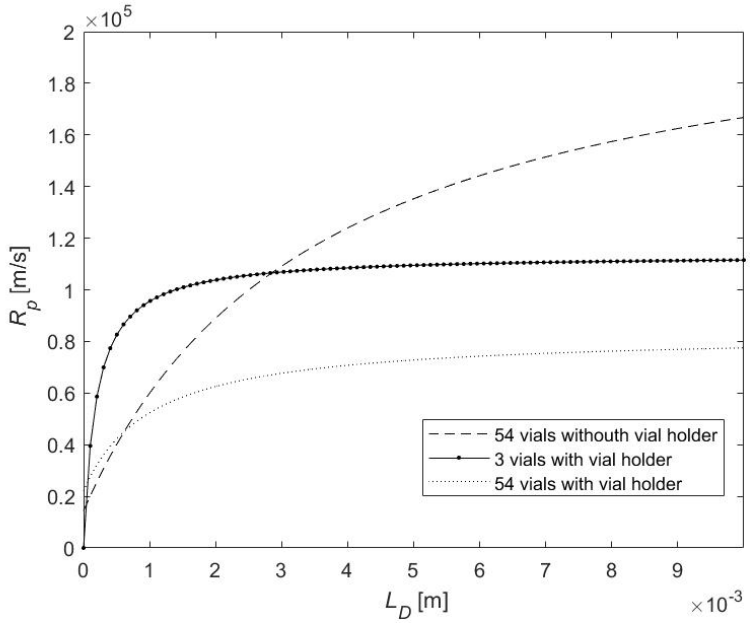

Figure 4.6 – R_p versus L_D for a 3% (w/w) sucrose solution freeze-dried at 10 Pa and -20 °C with three different experimental set-ups. for three experimental set-ups. Curves were obtained by fitting experimental data to equation 2.10.

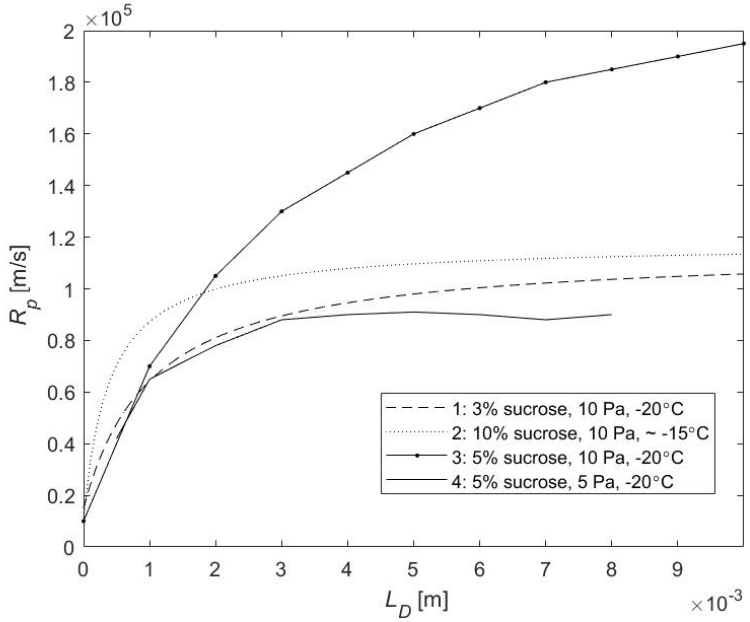

Figure 4.7 – Redrawn R_p versus L_D from other studies with various methods to estimate R_p. 1: Same method as in this study (Vanbillemont et al. 2020) 2: Used PRT with DPE (Giordano, Barresi, and Fissore 2011). 3: Used an algorithm based on product temperature measurements (Bosca, Barresi, and Fissore 2013). 4: Used PRT with DPE+ algorithm (Fissore and Pisano 2015).

From the set-up with 3 vials placed in the vial holder, it was possible to estimate the variability in the R_p measurement since five similar runs were performed. In table 4.3, the mean value and standard deviation of the coefficients $R_{P,0}$, A_{R_p}, and B_{R_p} are presented. Also included is the mean value and standard deviation of R_p at different values of dry layer thickness, L_D. As excepted, the variability in R_p is high with a relative error of around 10%. Compared to other studies where the uncertainty level of R_p has been estimated, the results presented in this report seems similar, although slightly higher (Mortier et al. 2016; Scutellà et al. 2018). Vanbillemont et.al (2020), who used the same method as in this study, estimated the standard deviation in R_p to $\sigma = 1.10{\cdot}10^4$ m/s. This is similar to the values presented in table 4.3.

Table 4.3 – Mean value and standard deviation, σ, of $R_{p,0}$, A_{R_p} and, B_{R_p} from five runs were 3 vials with 3% (w/w) sucrose solution were placed in a vial holder and freeze-dried at 10 Pa and -20°C. The mean and standard deviation of R_P at different values of L_D is also displayed.

	Mean	σ	unit
$R_{p,0}$	0.06	0.07	m/s
A_{R_p}	$6.0{\cdot}10^8$	$2.1{\cdot}10^8$	1/s
B_{R_p}	$5.3{\cdot}10^3$	$2.5{\cdot}10^3$	1/m
$R_{p,L_D=0.5mm}$	$8.2{\cdot}10^4$	$8.5{\cdot}10^3$	m/s
$R_{p,L_D=1.0mm}$	$9.7{\cdot}10^4$	$9.8{\cdot}10^3$	m/s
$R_{p,L_D=4.0mm}$	$1.1{\cdot}10^5$	$1.3{\cdot}10^4$	m/s
$R_{p,L_D=8.0mm}$	$1.1{\cdot}10^5$	$1.4{\cdot}10^4$	m/s

4.3 PRT for K_V and R_p determination

PRT-tests were successfully performed, however the determination of heat- and mass transfer coefficients from the PRT-data was not successful. This was due to the lack of speciality software to record the pressure rise during the pressure rise test. The freeze-dryer used during the experiments only records pressure at 5-second intervals, while speciality software can record pressure several times per second (Fissore, Pisano, and Barresi 2011b). Due to the low recording frequency, it was not possible to obtain robust fits to the MTM-equation (equation A.1), and hence, the parameter estimations were not possible to evaluate. In figure 4.8, three different fits to the same process data are shown to illustrate the problem.

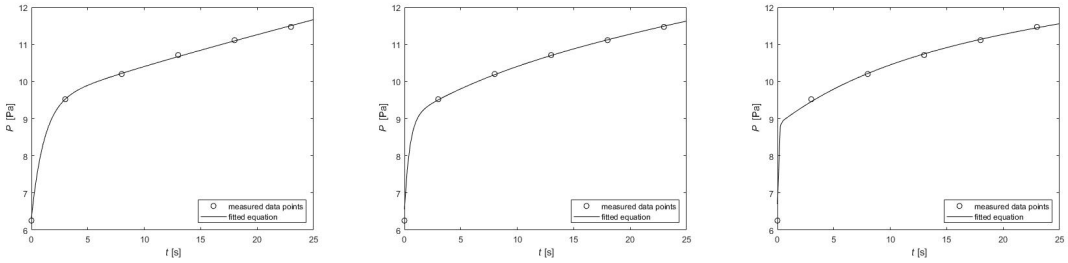

Figure 4.8 – Pressure rise tests conducted during freeze-drying at 6.25 Pa and -20°C, with fitted MTM equation. The figure shows the same fit performed three times to the same process data with different results.

4.4 Influence of Vial Holder Temperature

The result from the temperature measurements when 3 or 54 vials were placed in the vial holder and freeze-dried according to section 3.2 can be seen in figure 4.9.

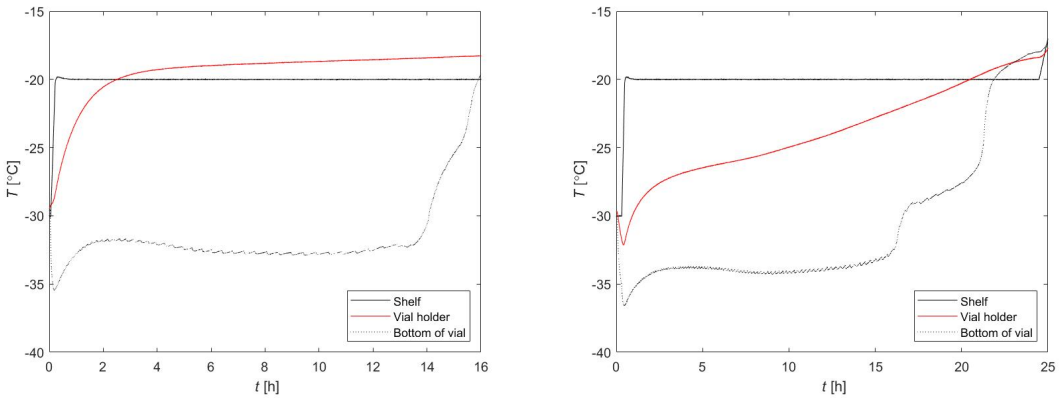

(a) 3 vials (b) 54 vials

Figure 4.9 – Temperature in the vial holder and at the bottom of the vials when vials with a 3% sucrose solution were placed in a vial holder and freeze dried at 10 Pa and -20°C. The shelf temperature is also included.

It is clear from figure 4.9 that using a different number of vials in the vial holder affects the temperature in the holder, and as a result, the product temperature at the vial bottom. While the temperature in the vial holder reaches the shelf temperature after around two hours of primary drying when 3 vials are used (figure 4.9a), it takes until the end of primary drying for the vial holder to reach shelf temperature when 54 vials are used (figure 4.9b). This is most likely due to the increased cooling-effect of 54 vials compared to 3 vials.

First of all, these results indicate that the assumption of steady state might be inadequate when using the vial holder, since it takes almost two hours for the system to reach somewhat stable temperatures, in the fastest case with 3 vials. Secondly, as a result of the cooling-effect from the vials, it is possible that K_V, when determined from the temperature difference between the shelf and the vial bottom will depend on the number of vials in the vial holder. Since K_V was determined for 54 vials, the cooling-effect from 54 vials is included in K_V, and it cannot be assumed that the same K_V is accurate for a different number of vials. By extension, this means that the determination of R_p for 3 vials in the vial holder might be inaccurate, since the K_V determined for 54 vials was used.

In order to estimate the heat transfer to the vials in a way that is independent from the number of vials in the vial holder, a possibility is to base the heat transfer coefficient on the temperature difference between the vial holder and the bottom of the vial, instead of the difference between shelf and vial. From now on, such a coefficient is called $K_{V,vh}$ [W/m^2· K], and the temperature in the vial holder is called T_{vh} [K]. Since T_{vh} was measured during one of the runs at 10 Pa when K_V was determined, this measurement was used to determine $K_{V,vh}$ at 10 Pa to 52 W/m^2· K (compared to K_V = 29 W/m^2·K at 10 Pa when the vial holder is used).

With $K_{V,vh}$ known, R_p could be calculated based on the temperature in the vial holder for the runs with 3 and 54 vials placed in the vial holder. In figure 4.10 R_p has been estimated both from the vial holder temperature (using $K_{V,vh}$) and from the shelf temperature (using K_V). As expected, for 54 vials the plateau value of R_p is the same whether it was estimated from T_S or T_{vh}. For 3 vials however, the R_p estimation based on vial holder temperature was significantly lower than the estimation based on shelf temperature.

These results explain the contradiction between the R_p results discussed in section 4.2 and the theory that higher product temperature gives less resistance to vapour flow due to increased microcollapse. Now, when R_p is estimated from the temperature in the vial holder, the case with 3 vials in vial holder has the lowest R_p. This is also the case with the higher product temperature, and were the most collapse was observed (figure 4.5). A comparison between R_p and observed cake collapse can be seen in figure 4.11. Another difference between the R_p estimations based on T_S and T_{vh} is that the sharp maximum and following decrease in R_p can be seen for both 3 and 54 vials when R_p is estimated from T_{vh}.

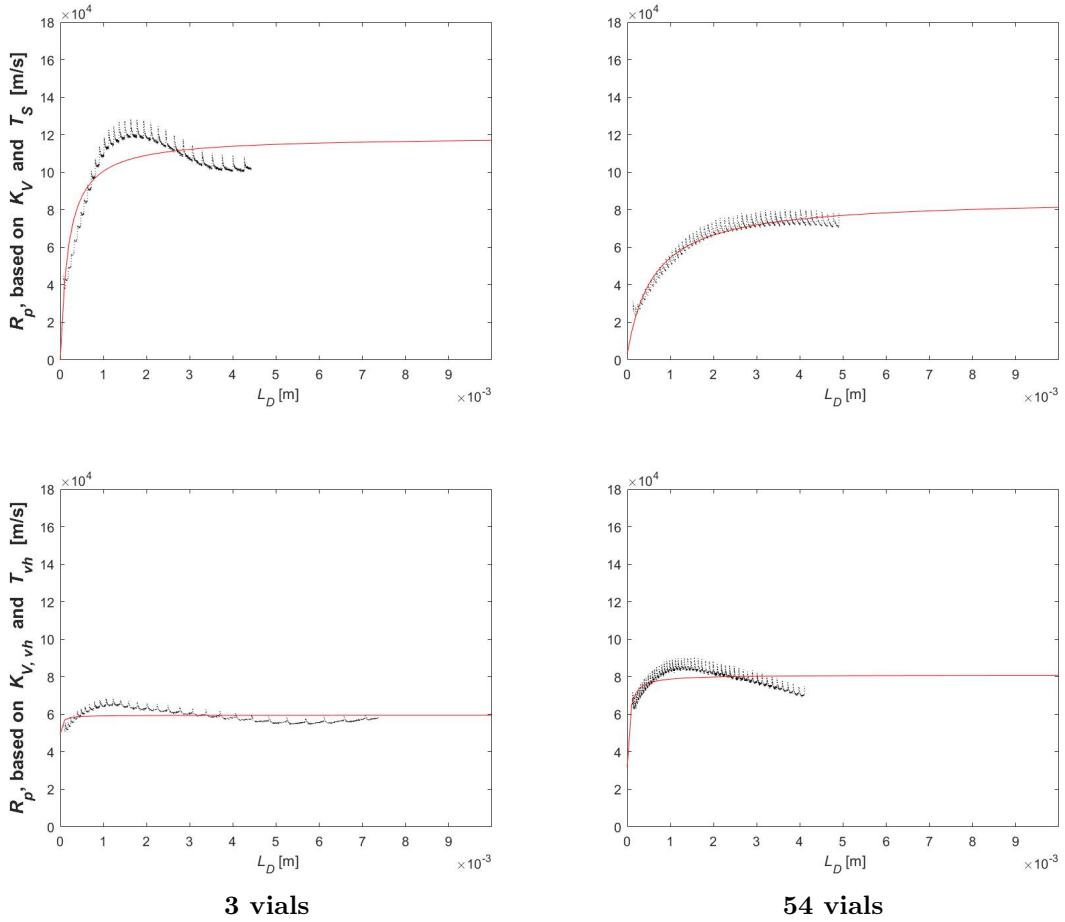

Figure 4.10 – R_p for 3% (w/w) sucrose solution estimated from shelf- and vial holder temperature for 3 and 54 vials placed in vial holder and freeze-dried at 10 Pa and -20°C. The dotted line is the R_p estimation based on product temperature measurements, and the red line is the fit to equation 2.10. In the upper figures, R_p is estimated from the shelf temperature, and in the lower figures, R_p is estimated from the vial holder temperature.

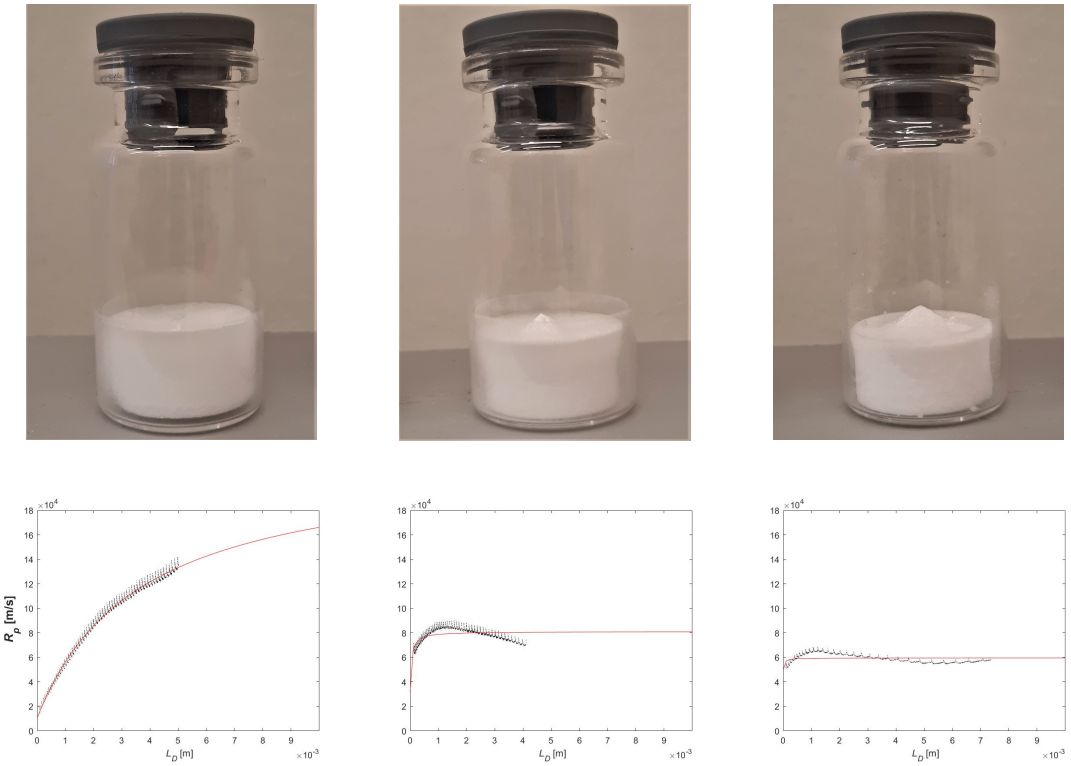

54 vials without vial holder | 54 vials in vial holder | 3 vials in vial holder

Figure 4.11 – Comparison between observed cake collapse and measured R_p based on product temperature measurements. Vials were placed either directly on the shelf, or in a vial holder and freeze-dried at 10 Pa and -20 °C. For the vials placed in vial holder, R_p was estimated from the vial holder temperature, T_{vh}. Dotted line is the measured R_p, and the red line is the fit to equation 2.10.

4.5 Model Verification

In table 4.4, the model predictions and actual drying times for the verification runs are presented. Note that the model uses K_V values presented in section 4.1, and not $K_{V,vh}$.

Table 4.4 – Model predictions and verification runs of primary drying time for freeze-drying of 3 ml 3% (w/w) sucrose solution at 10 Pa and -20°C.

Case	Model prediction	Verification run	Difference
54 vials placed directly on shelf	19 h 58 min	17 h 10 min	2 h 48 min
3 vials in vial holder	12 h 12 min	13 h 7 min	1 h 5 min

In the case of 54 vials placed directly on the shelf, the model overestimated the drying time with 14%. For 3 vials in vial holder, the model instead underestimated the drying time with 9%.

For 3 vials in holder, there are two reasons why there would be differences between model prediction and actual drying time. Firstly, that the model and model parameters does not accurately describe the freeze-drying process, and secondly, the intrinsic vial-to-vial variability. One approach to improve the performance of the simulation and to minimize the difference between simulation and actual drying is to take measures to control the nucleation process during freezing. Controlling the freezing process means less variability between vials, and potentially also better model parameter estimations since the intrinsic variability is minimized.

For 54 vials placed directly on the shelf, the difference in drying behaviour between vials with thermocouples and other vials of the batch adds another error source. Since the model parameters K_V and R_p are determined from temperature measurements, they describe the behaviour of vials with thermocouples. They dry faster than the rest of the batch, which means that the simulation should underestimate the drying time for the whole batch, unless the model is adjusted to accommodate this difference in drying time. Based on the R_p-determination runs for 54 vials placed directly on the shelf, the difference between model prediction and actual drying time was estimated to 5 hours. 5 hours were therefore added to the model when estimating the drying time for 54 vials on the shelf. Based on the results presented

in table 4.4, 5 hours might have been an overestimation. The fact remains, that the difficulty of estimating the difference in drying behaviour between vials with thermocouples and other vials of the batch, makes it hard to model the freeze-drying of a complete batch and make accurate predictions of drying time.

It must be noted that only one verification run for each case was performed, and that more verification runs are needed in order to ensure that the results presented here are not outliers.

The model prediction of temperature, and the actual temperatures measured during the verification runs are presented in figure 4.12. For both cases, it can be seen that the temperature at the start of primary drying is underestimated by the model. However, for 54 vials, the measured temperature was very close to the model prediction for the first 4 hours or primary drying, after which it plateaued at a lower temperature than predicted by the model. For 3 vials, the measured temperature did not follow the model prediction as closely. It should be noted that the simulation of 3 vials placed in the vial holder was based on the K_V value determined from 54 vials and shelf temperature, and not vial holder temperature. This could be a reason for the inadequate temperature prediction.

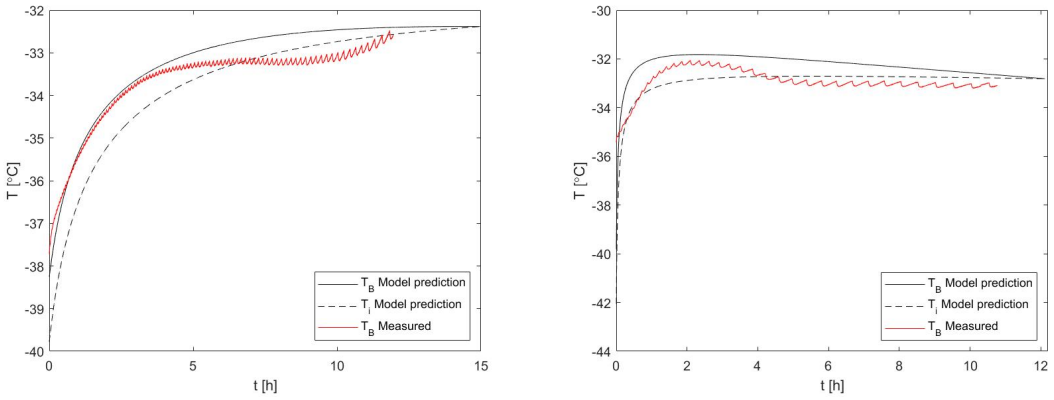

Figure 4.12 – Comparison of model prediction and measured temperature for freeze-drying of a 3 ml 3% (w/w) sucrose solution at 10 Pa and -20°C. when 54 vials are placed directly on the shelf (a) and 3 vials are placed in vial holder (b).

An interesting observation is that in both cases, the accuracy of the model prediction is significantly decreased at the onset of temperature decrease as a result of microcollapse. It becomes evident that the used model is incapable of describing the occurrence of microcollapse. Therefore, an interesting approach to improve model performance would be to describe the relationship between R_p and L_D in two intervals with one equation for the part before microcollapse, and one after, as discussed in section 4.2.

The model in itself can also be improved. In the simulation, shelf temperature and chamber pressure are set to their final values during primary drying. The start of primary drying, where the pressure is lowered and the temperature increased is not included. As the sublimation process starts during the pressure decrease, the model used in the simulation does not accurately describe the start of the drying-process. There are several examples in literature of similar models including the start-up phase of the primary drying (Mortier et al. 2016; Vanbillemont et al. 2020). For example, this could be the reason why the predicted temperature at the beginning of primary drying is much lower than the measured temperature. However, including the start-up of primary drying in the model is not excepted to affect the drying time prediction to any large extent, since the start-up phase is only around 10 minutes in duration.

5 Conclusion

The objective of this thesis work was to:

- determine mass- and heat transfer parameters for the primary drying of pharmaceutcial vial freeze-drying.
- investigate the influence of using a vial holder when freeze-drying.
- model primary drying to predict drying time and product temperature.

From the work reported in this paper it is concluded that the dry layer resistance, R_p, can be adequately estimated by measuring product temperature at the vial bottom and using a heat conduction model. However, the variation in R_p is high, which makes it difficult to estimate accurately from a single measurement. Additionally, equations often used in literature to describe the relationship between R_p and dry layer thickness are not accurate when microcollapse occurs. The overall heat transfer coefficient, K_V, can be reliably determined by the gravimetric method.

It is further concluded that using an aluminum vial holder increases temperature homogeneity during freeze-drying. It does however also affect the heat transfer and dry layer resistance in ways not fully understood. For example, the number of vials in the vial holder seems to play a role, and the steady state assumption can be questioned. When it comes to the heat transfer, above 7.3 Pa the heat transfer to the vials is higher and below 2 Pa lower, when using a full vial holder as compared to when no vial holder is used.

Simulation of primary drying with a one-dimensional steady state model has the potential of providing good estimations of product temperature and drying time if improvements suggested in this work are implemented.

6 Future Work

In future, there are several interesting aspects to investigate further in order to improve the estimation of K_V and R_p, and to be able to accurately model a complete freeze-drying batch with good accuracy.

Measures to control the freezing behaviour should be investigated as a potential way of minimizing vial-to-vial and batch-to-batch variability. However, the problem with thermocouple interference remains, and it would therefor be interesting to estimate the actual impact of the thermocouple further. For example by estimating R_p and K_v non-invasively and compare with the estimations in this work. It should also be investigated if it is possible to measure product temperature with other methods.

The model used to simulate the primary drying process should also be improved. For example by including the start-up phase of primary drying in the model, and by describing R_p in a way that better applies to the case of microcollapse.

In order to expand the understanding of the dry layer resistance behaviour, it would also be interesting to measure R_p for a wider range of formulations and process conditions. For example R_p could be measured for different concentrations, for different types of formulations and at different process conditions. It would also be interesting to relate the R_p measurements to the visual structure of the dry cake, for example investigated with scanning electron microscopy or transmission electron microscopy.

References

Bosca, S., A. A. Barresi, and D. Fissore (2013). "Use of a soft sensor for the fast estimation of dried cake resistance during a freeze-drying cycle". In: *International Journal of Pharmaceutics* 451 (1–2), pp. 23–33. DOI: https://doi.org/10.1016/j.ijpharm.2013.04.046.

Fissore, D. and R. Pisano (2015). "Computer-Aided Framework for the Design of Freeze-Drying Cycles: Optimization of the Operating Conditions of the Primary Drying Stage". In: *Processes* 3 (2), pp. 406–421. DOI: https://doi.org/10.3390/pr3020406.

Fissore, D., R. Pisano, and A. A. Barresi (2011a). "Advanced Approach to Build the Design Space for the Primary Drying of a Pharmaceutical Freeze-Drying Process". In: *Journal of Pharmaceutical Sciences* 100 (11), pp. 4922–4933. DOI: https://doi.org/10.1002/jps.22668.

— (2011b). "On the Methods Based on the Pressure Rise Test for Monitoring a Freeze-Drying Process". In: *Drying Technology* 29, pp. 73–90. DOI: https://doi.org/10.1080/07373937.2010.482715.

Franks, F. and T. Auffret (2007). *Freeze-drying of Pharmaceuticals and Biopharmaceuticals: Principles and Practice*. Royal Society of Chemistry. ISBN: 978-1-84755-770-4.

Giordano, A., A. A. Barresi, and D. Fissore (2011). "On the use of mathematical models to build the design space for the primary drying phase of a pharmaceutical lyophilization process". In: *Journal of Pharmaceutical Science* 100 (1), pp. 311–324. DOI: https://doi.org/10.1002/jps.22264.

Kharaghani, A. et al. (2017). "Freeze-Drying". In: *Ullmann's Encyclopedia of Industrial Chemistry*. John Wiley Sons, Inc.

Kuu, W. Y., L. M. Hardwick, and M. J. Aker (2006). "Rapid determination of dry layer mass transfer resistance for pharmaceutical formulations during primary drying using product temperature profiles". In: *International Journal of Pharmaceutics* 313 (1-2), pp. 99–113. DOI: https://doi.org/10.1016/j.ijpharm.2006.01.036.

Mortier, S. T. F. C. et al. (2016). "Uncertainty analysis as essential step in the establishment of the dynamic Design Space of primary drying during freeze-drying". In: *European Journal of Pharmaceutics and Biopharmaceutics* 103, pp. 71–83. DOI: https://doi.org/10.1016/j.ejpb.2016.03.015.

Murphy, D. M. and T. Koop (2005). "Review of the vapour pressures of ice and supercooled water for atmoshperic applications". In: *Quarterly Journal of the Royal Meteorological Society* 131 (608), pp. 1539–1565. DOI: https://doi.org/10.1256/qj.04.94.

Patel, S., S. Chaudhuri, and M. J. Pikal (2010). "Choked flow and importance of Mach I in freeze-drying process design". In: *Chemical Engineering Science* 65

(21), pp. 5716–5727. DOI: https://doi.org/10.1016/j.ces.2010.07.024.

Pikal, M. J. (1985). "Use of Laboratory Data in Freeze Drying Process Design: Heat and Mass Transfer Coefficients and the Computer Simulation of Freeze Drying". In: *PDA Journal of Pharmaceutical Science and Technology* 39 (3), pp. 115–139.

Pikal, M. J., M. L. Roy, and S. Shah (1984). "Mass and heat transfer in vial freeze-drying of pharmaceuticals: Role of the vial". In: *Journal of Pharmaceutical Science* 73 (9), pp. 1224–1237. DOI: https://doi.org/10.1002/jps.2600730910.

Pisano, R. et al. (2013). "Quality by design: optimization of a freeze-drying cycle via design space in case of heterogeneous drying behaviour and influence of freezing protocol". In: *Pharmaceutical Development and Technology* 18 (1), pp. 280–295. DOI: https://doi.org/10.3109/10837450.2012.734512.

RISE (2020). *Bättre biologiska läkemedel*. https://www.ri.se/sv/battre-biologiska-lakemedel. Accessed: 2021-05-15.

Scutellà, B. et al. (2018). "Determination of the dried product resistance variability and its influence on the product temperature in pharmaceutical freeze-drying". In: *European Journal of Pharmaceutics and Biopharmaceutics* 128, pp. 379–388. DOI: https://doi.org/10.1016/j.ejpb.2018.05.004.

Tang, X. C., S. L. Nail, and M. J. Pikal (2006a). "Evaluation of manometric temperature measurement, a process analytical technology tool for freeze-drying: part I, product temperature measurement". In: *AAPS PharmSciTech* 7 (1), E14. DOI: https://doi.org/10.1208/pt070114.

— (2006b). "Evaluation of manometric temperature measurement, a process analytical technology tool for freeze-drying: part II, measurement of dry layer resistance". In: *AAPS PharmSciTech* 7 (4), p. 93. DOI: https://doi.org/10.1208/pt070493.

— (2006c). "Evaluation of manometric temperature measurement, a process analytical technology tool for freeze-drying: part III, heat and mass transfer measurement". In: *AAPS PharmSciTech* 7 (4), p. 97. DOI: https://doi.org/10.1208/pt070497.

Tchessalov, S. et al. (2021). "Application of First Principles Primary Drying Model to Lyophilization Process Design and Transfer: Case Studies From the Industry". In: *Journal of Pharmaceutical Science* 110 (2), pp. 968–981. DOI: https://doi.org/10.1016/j.xphs.2020.11.013.

Vanbillemont, B. et al. (2020). "Model-Based Optimisation and Control Strategy for the Primary Drying Phase of a Lyophilisation Process". In: *Pharmaceutics* 12 (2), p. 181. DOI: https://doi.org/10.3390/pharmaceutics12020181.

A Appendix

A.1 MATLAB Function for Simulation of Primary Drying

```
function [t_ans, Ti_ans, dT_ans, Pi_ans, dmdt_ans, Ld_ans,
    Rp_ans, msubTot_ans] = freezeDry(P, T, V, Rp0, ARp, BRp,
    KV)

%Simulation of primary drying with Martin Christ Epsilon 2-6
    D LCS plus
%freeze-drying and Scott VCDIN tubing vials. Takes imput
    arguments chamber
%pressure P [Pa], shelf temperature T [ C ] fill volume V [
    ml], and
%determined parameters for Rp, Rp0 [m/s], ARp [1/s] and BRp
    [1/m]. KV
%should have the value 0, 1 or 2 and denotes the heat
    transfer case
% 0 = simulation of non-edge vials when freeze-drying
    without vial holder
% 1 = simulation of edge vials when freeze-drying without
    vial holder
% 2 = simulation of freeze-drying with vial holder


%% In arguments

Pc = P; % Pa % Set chamber pressure
Ts = T + 273.15; % K % Set shelf temperature

%% At start
Ld = 0; % m %dry layer thickness
```

```
20 dmdt = 0; % kg /s % sublimation rate
21 msubTot = 0; % mass of total sublimated water
22
23 %Start-values [Ti dHsub dT Pi]
24 Guess = [237.15; 2.8421e+06; 2; 10]; % Guess initial values
       of Ti, dHsub, dT, Pi for solver
25
26 %% Constants
27 M = 0.0180; %kg/mol Molar mass of water
28 ri = 0.011; %m inner vial radius
29 ro = 0.012; %m outer vial radius
30 Ap = pi.*ri^2 ; %m2 %product cross section area, based on
       inner vial radius
31 Av = pi.*ro^2 ; %m2 % vial cross section area, based on
       outer vial radius
32 Ltot = totalThickness(V); %m
33
34
35 %% Heat and mass transfer parameters
36
37 if KV == 0
38     Kv = Kv_noHolder(Pc,0); % non-edge
39 elseif KV == 1
40     Kv = Kv_noHolder(Pc,1); % edge
41 elseif KV == 2
42     Kv = Kv_holder(Pc); % vialholder
43 end
44
45 Rp = Rp0 + ARp.*Ld./(1+BRp*Ld); % m/s
46
47 %% Time interval
48
49 t_start = 0; %s
50 dt = 5; %s
51 t_stop = 3600 *24; %s
```

```
52
53 %% Create answer vectors of right size
54
55 Ti_ans = zeros(1,t_stop/dt +1);
56 dT_ans = zeros(1,t_stop/dt +1);
57 Pi_ans = zeros(1,t_stop/dt +1);
58 t_ans = linspace(t_start,t_stop,t_stop/dt+1);
59 dmdt_ans = zeros(1,t_stop/dt +1);
60 Ld_ans = zeros(1,t_stop/dt +1);
61 Rp_ans = zeros(1,t_stop/dt +1);
62 msubTot_ans = zeros(1,t_stop/dt +1);
63
64
65 %% Solve interdependent equations
66 n = 1; % count
67 for i = t_start:dt:t_stop
68
69 syms Ti dHsub dT Pi
70 S = [Ti, dHsub, dT, Pi];
71 F = @(S) [-exp(9.550426-5723./S(1) + 3.53068.*log(S(1))
       -0.00728.*S(1))+(Ap*S(2)*Pc + Av*Kv*Rp*Ts -Av*Kv*Rp*S(1)
      + Av*Kv*Rp*S(3))./(Ap*S(2));
72 -S(3)+(889200*(Ltot - Ld).*(S(4)-Pc)./Rp-0.0102.*(Ltot-Ld)
       .*(Ts-S(1)))./(1-0.0102*(Ltot-Ld));
73 -S(2) + (4.68.*10^4+35.9.*S(1)-0.0741.*S(1)^2+542.*exp(-(S
       (1)./124)^2))./M;
74 -S(4)+ exp(9.550426-5723./S(1) + 3.53068.*log(S(1))
       -0.00728.*S(1));];
75
76 % x = [Ti dHsub dT Pi]
77 x = fsolve(F,Guess);
78
79 msub = dmdt*dt; % kg mass of sublimated water during last
      timestep
80 msubTot = msubTot + msub; % kg mass of total sublimated
```

```
    water
Ld = Ld + dryLayer(msub); % total thickness of dry layer
dmdt = Ap.*(x(4)-Pc)./Rp; % Sublimation rate kg/s
Rp = Rp0 + ARp.*Ld./(1+BRp*Ld);

if Ld > Ltot % Primary drying is completed
    break
end

Ti_ans(n) = x(1);
dT_ans(n) = x(3);
Pi_ans(n) = x(4);
dmdt_ans(n) = dmdt;
Ld_ans(n) = Ld;
Rp_ans(n) = Rp;
msubTot_ans(n) = msubTot;

Guess = [x(1); x(2); x(3); x(4)];

n = n+1;
end

end
```

A.2 MATLAB Function for Determination of R_p

```
function [RpCoef, Ld, Ld_fit, Rp, Rp_fit, Ti, Pi, t_dry,
    P_dry, rsub] = estimateRp(pData, V_fill, Pc, KV, Tf,
    startOfSublimationGuess, endRow)
% Estimate Rp based on recorded process data and a heat
    conduction model.
% pData is matrix with recorded process data:
% Column 1: duration [s]
% Column 2: chamber pressure [mBar]
% Column 3: shelf temperature [ C ]
% Column 4: product temperature 1
% Column 5: product temperature 2
% Column 6: product temperature 3
% Column 7: mean product temperature

% V_fill is fill volume [ml]. Pc is set chamber pressure [Pa
    ], Tf is
% product temperature at the end of the freezing step.
% startOfSublimationGuess is a vector [a b] where a-b is the
     interval of
% rows in pData were the start of sublimation is believed to
     be. Needs to
% be quite accuarate (within 100-200 rows). endRow is the
    row in pData were
% the Rp-estimation should stop (because the thermocouple
    has lost contact
% with the frozen layer)


% KV should have the value 0, 1 or 2 and denotes the heat
    transfer case
% 0 = simulation of non-edge vials when freeze-drying
    without vial holder
% 1 = simulation of edge vials when freeze-drying without
    vial holder
```

```
% 2 = simulation of freeze-drying with vial holder

%% Assignment of in-argument
Tb = pData(:,7) + 273.15; % K
Ts = pData(:,3) + 273.25; % K
t = pData(:,1); % s
P = pData(:,2).*100; % Pa

%% Constants
dH = 2.84*10^6; % J/kg
cond = 2.23; %W/m K thermal conductivity of ice
ri = 0.011; %m inner vial radius
ro = 0.012; %m outer vial radius
Ap = pi.*ri^2 ; %m2 %product cross section area, based on
    inner vial radius
Av = pi.*ro^2 ; %m2 % vial cross section area, based on
    outer vial radius
Lt = totalThickness(V_fill); %m % Total thickness
% vial heat transfer coefficient
if KV == 0
    Kv = Kv_noHolder(Pc,0); % non-edge
elseif KV == 1
    Kv = Kv_noHolder(Pc,1); % edge
elseif KV == 2
    Kv = Kv_holder(Pc); % vialholder
end

%% At start
Ld_temp = 0; %m % Thickness of dry layer at start
Lf = Lt; %m % Thickness of frozen layer at start
msub = 0; % kg mass of sublimated water at start

%% Kollar n r det b rjar sublimera
for i = startOfSublimationGuess(1):1:startOfSublimationGuess
    (2)
```

```
56      Ti_temp = Tf+273.15; %K = temperaturen vid slutet av
            frysningen
57      Pi = exp(9.550426-5723./Ti_temp + 3.53068.*log(Ti_temp)
            -0.00728.*Ti_temp); % Pa
58
59      if Pi > P(i)
60          startOfSublimationTime = t(i); %
61          startOfSublimationRow = i;
62
63          break
64      end
65  end
66  %% Calculates Ti, Pi, rsub, Rp....
67
68  % creating answer vectors
69  rsub = [];
70  Ti = [];
71  t_dry = [];
72  P_dry = [];
73  Lf_ans = [];
74  Pi = [];
75  Rp = [];
76  Ld = [];
77
78  for i = startOfSublimationRow:1:endRow
79  Kv = Kv_holder(P(i)); % vial heat transfer coefficient W/m2
        K for vialholder
80  Ti_temp = Tb(i) - (Ts(i)-Tb(i)).*Kv.*Lf./cond; % K
81  Pi_temp = exp(9.550426-5723./Ti_temp + 3.53068.*log(Ti_temp)
        -0.00728.*Ti_temp); % Pa
82
83  rsub_temp = Av.*Kv.*(Ts(i)-Tb(i))./dH; % kg/s % sublimation
        rate
84  dt = t(i)-t(i-1); %s
85  msub = rsub_temp*dt; % kg mass of sublimated water during
```

```
    last timestep
Ld_temp = Ld_temp + dryLayer(msub); % total thickness of dry
    layer
Lf = Lt-Ld_temp;  % remaining thickness of ice
Rp_temp = (Pi_temp-P(i)).*Ap./rsub_temp; %m/s

rsub = [rsub, rsub_temp];
Ti = [Ti, Ti_temp];
t_dry = [t_dry, t(i)];
P_dry = [P_dry, P(i)];
Lf_ans = [Lf_ans, Lf];
Pi = [Pi, Pi_temp];
Rp = [Rp, Rp_temp];
Ld = [Ld, Ld_temp];
end

%% Fit Rp curve with lsqcurvefit
R0 = 1.4*10^4; % initial guess
A = 2.1*10^8; %initial guess
B = 1300; % initial guess

Ld_fit = Ld(120:end);
Rp_fit = Rp(120:end);

coef0 = [R0, A, B];
lb = [0, 1*10^4, 0];
ub = [5*10^4, 1*10^9, 10000];

fun = @(coef,x)coef(1) + coef(2).*x./(1+coef(3).*x);
RpCoef = lsqcurvefit(fun,coef0,Ld_fit,Rp_fit,lb,ub);

end
```

A.3 Manometric Temperature Measurment (MTM)

The equations used by MTM to describe the pressure rise during a PRT is shown in equation A.1. The equation assumes four reasons behind the pressure rise (Fissore, Pisano, and Barresi 2011b):

1. sublimation of ice controlled by dry layer resistance and temperature at the sublimation interface.
2. increased temperature at the sublimation interface arising from dissipation of the temperature gradient over the frozen layer during the PRT.
3. increased temperature at the sublimation interface due to heat transfer from the shelf during the PRT.
4. air leaks to the drying chamber.

$$P_C(t) = P_i - (P_i - P_0)e^{-Kt} + \frac{P_i \Delta H_{sub}}{RT_i^2}\frac{\Delta T_i}{2}\left(1 - \frac{8}{\pi^2}e^{-\frac{\lambda_{ice}\pi^2}{\rho_{ice}C_{p,ice}L_{frozen}}t}\right) \tag{A.1}$$

$$+\left[\frac{P_i \Delta H_{sub}}{RT_i^2}\frac{1}{\rho_{ice}C_{p,ice}L_{frozen}}K_V(T_S - T_B)\right]t + F_{leak}t$$

where
$T_B = T_i + \Delta T$
and
$K = \frac{N_V A_p R T_C}{M_W V_C R_p}$